Today’s Agenda

- 2D Fourier Transform
- Filtering in Frequency domain

DFT of this Function:

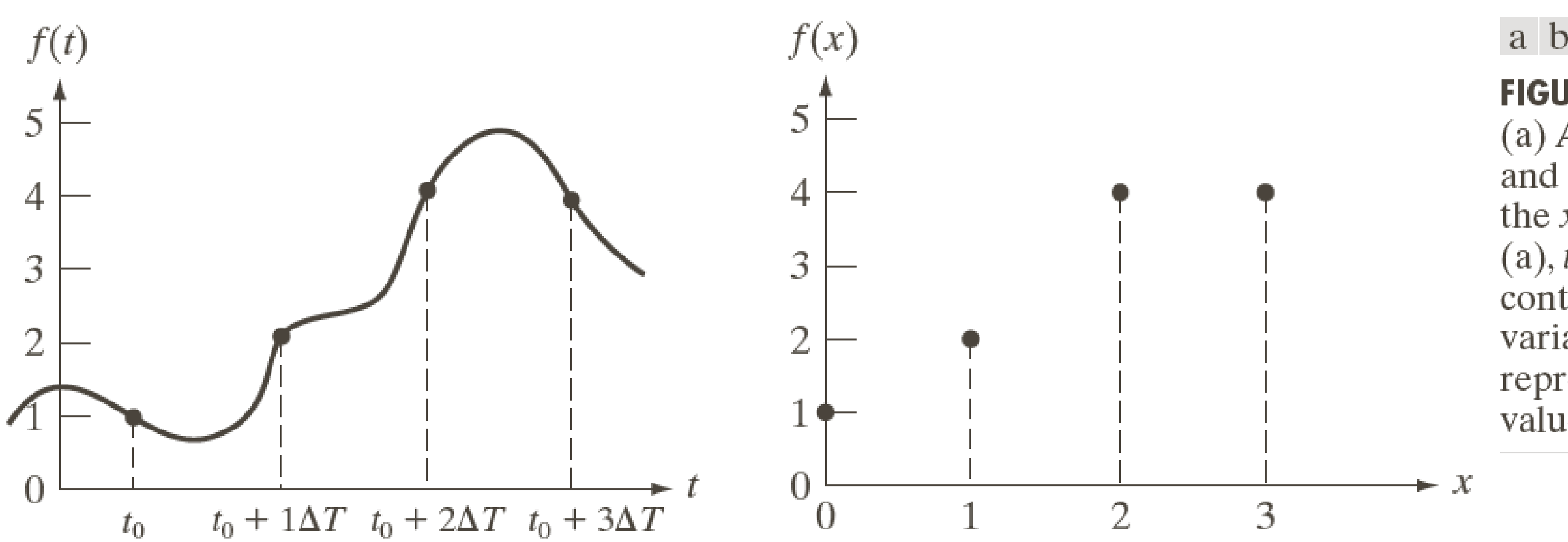

FIGURE 4.11 (a) A function, and (b) samples in the x-domain. In (a), t is a continuous variable; in (b), x represents integer values.

$$F(0) = \sum_{x=0}^{3} f(x) = 1 + 2 + 4 + 4 = 11$$

$$F(1) = ?,\ F(2) = ?,\ F(3) = ?$$

FT, FS, DTFT, DFT

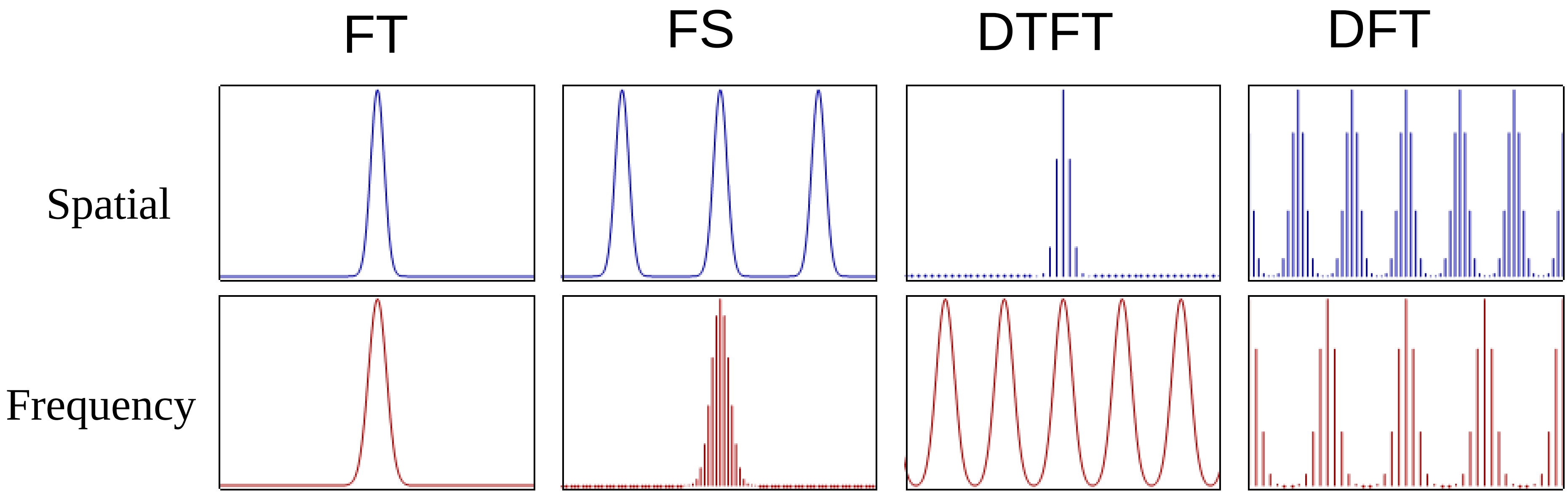

https://en.wikipedia.org/wiki/Discrete_Fourier_transform#/media/File:From_Continuous_To_Discrete_Fourier_Transform.gif

Extension to 2D Fourier Transform

$$F(\mu,\nu) = \int_{-\infty}^{\infty}\int_{-\infty}^{\infty} f(t,z)e^{-j2\pi(\mu t+\nu z)}dtdz$$

$$f(t,z) = \int_{-\infty}^{\infty}\int_{-\infty}^{\infty} F(\mu,\nu)e^{j2\pi(\mu t+\nu z)}d\mu d\nu$$

2D Step Function and FT

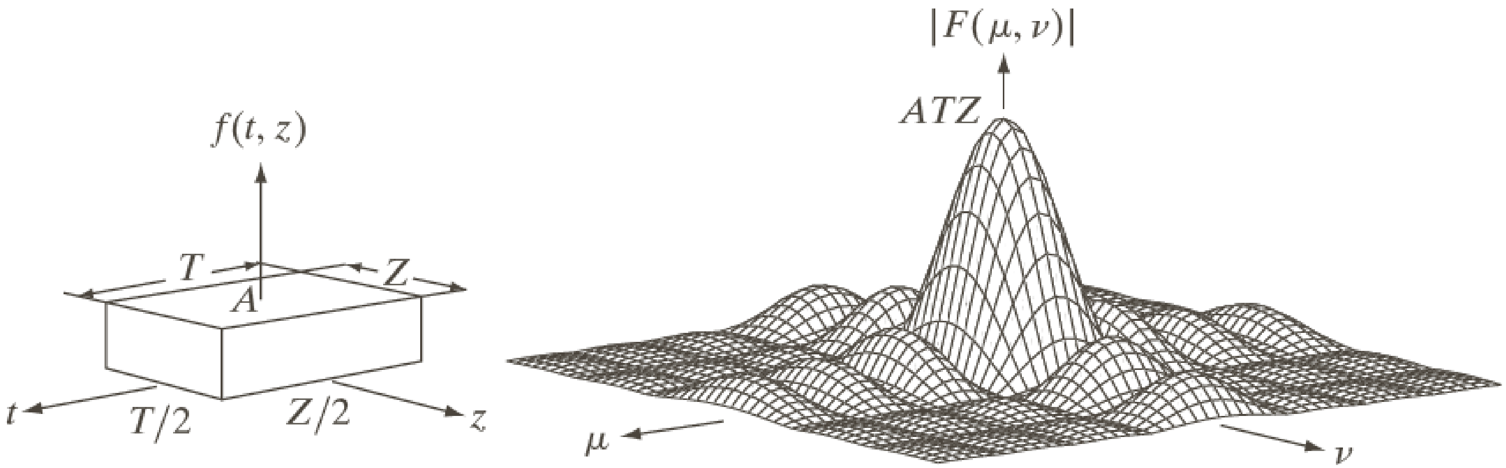

FIGURE 4.13 (a) A 2-D function, and (b) a section of its spectrum (not to scale). The block is longer along the t-axis, so the spectrum is more "contracted" along the μ-axis. Compare with Fig. 4.4.

$$F(\mu, \nu) = ATZ\left[\frac{\sin(\pi\mu T)}{(\pi\mu T)}\right]\left[\frac{\sin(\pi\nu Z)}{(\pi\nu Z)}\right]$$

Extension to 2D Fourier Transform

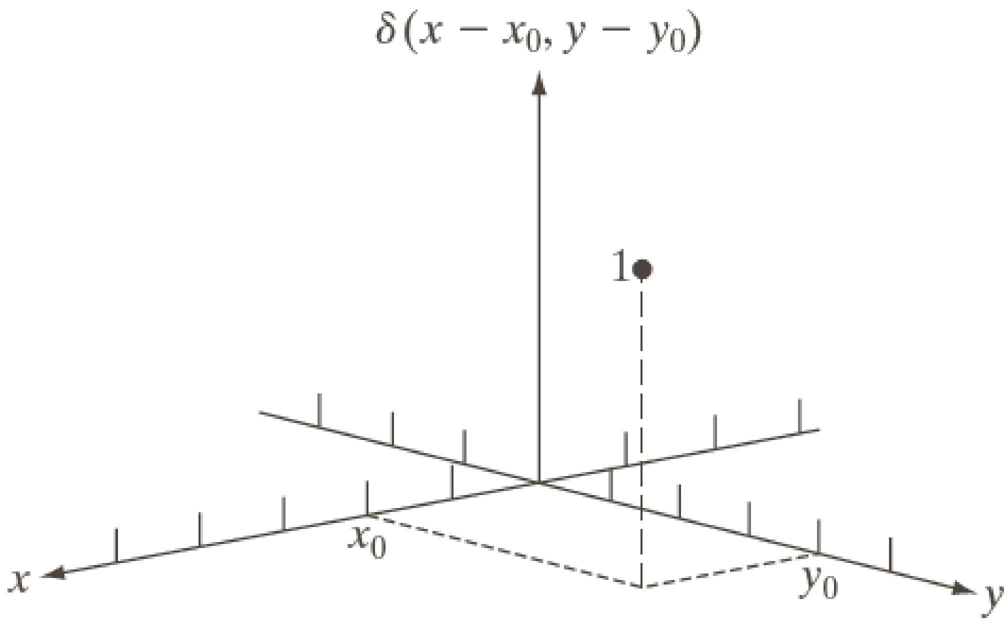

FIGURE 4.12 Two-dimensional unit discrete impulse. Variables x and y are discrete, and δ is zero everywhere except at coordinates (x_0, y_0).

2D Sampling

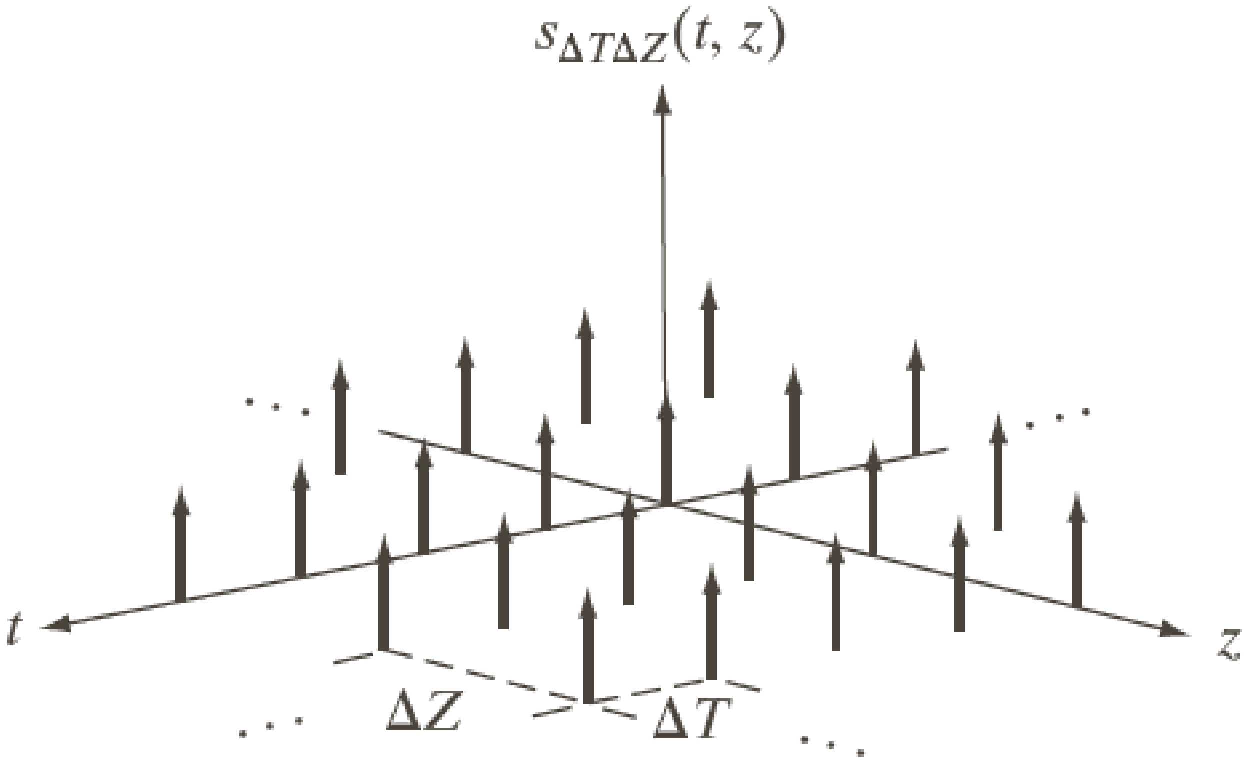

FIGURE 4.14 Two-dimensional impulse train.

$$S_{\Delta T \Delta Z}(t, z) = \sum_{m=-\infty}^{\infty} \sum_{n=-\infty}^{\infty} \delta(t - m\Delta T, z - n\Delta Z)$$

Aliasing in 2D

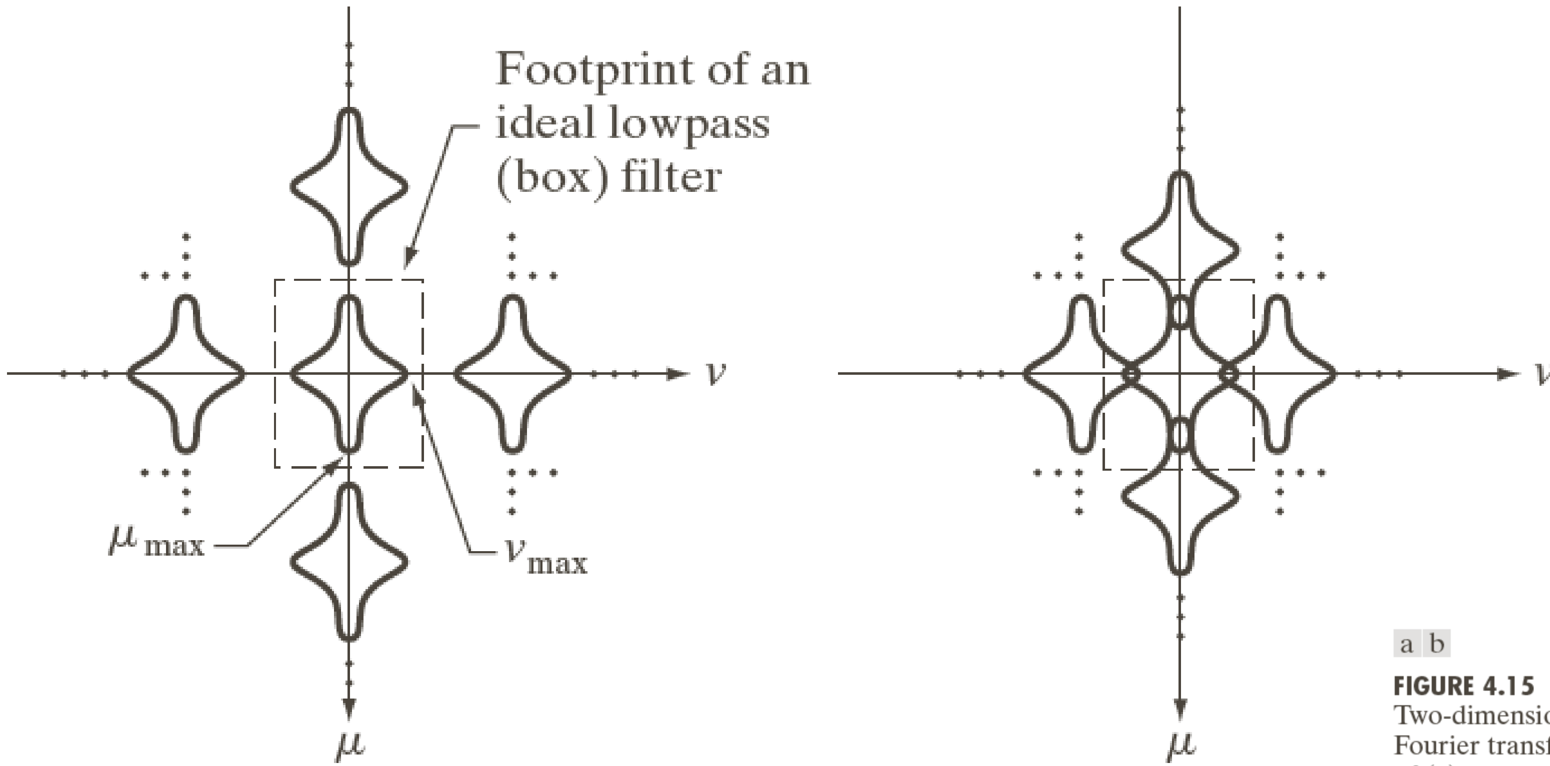

FIGURE 4.15 Two-dimensional Fourier transforms of (a) an over-sampled, and (b) under-sampled band-limited function.

Aliasing Examples

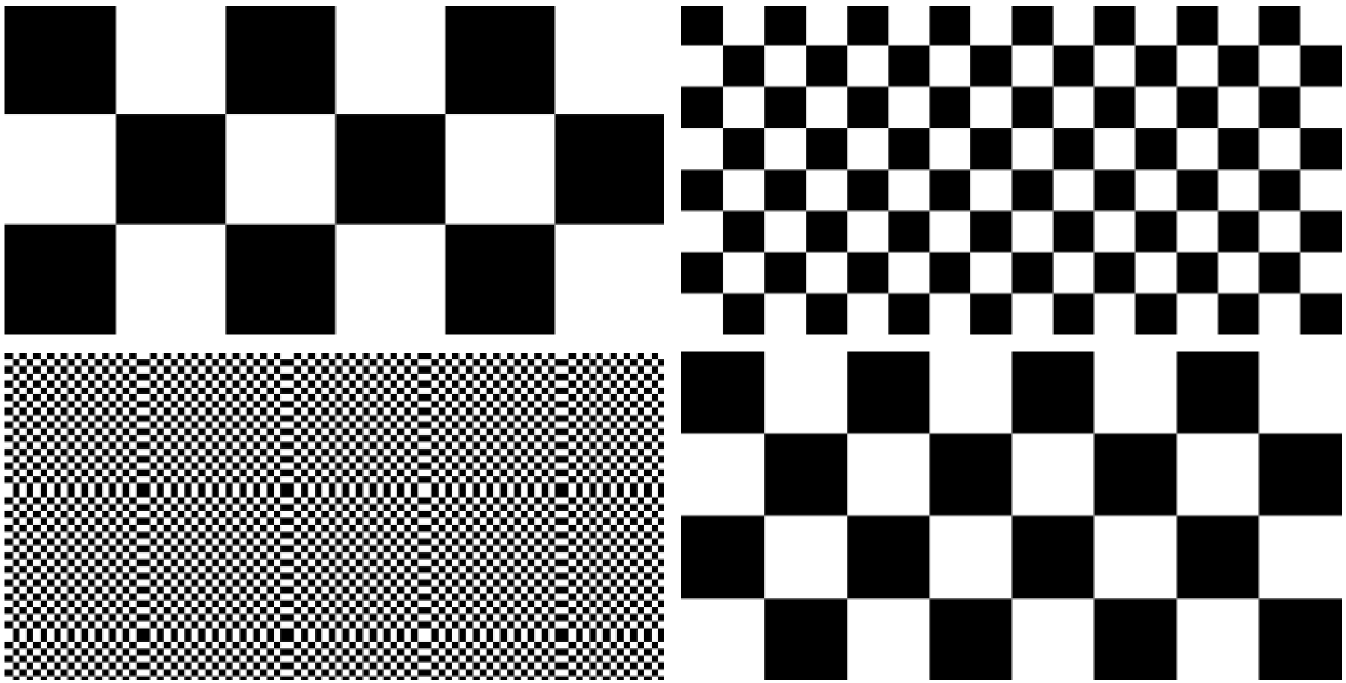

a b
c d

FIGURE 4.16 Aliasing in images. In (a) and (b), the lengths of the sides of the squares are 16 and 6 pixels, respectively, and aliasing is visually negligible. In (c) and (d), the sides of the squares are 0.9174 and 0.4798 pixels, respectively, and the results show significant aliasing. Note that (d) masquerades as a "normal" image.

Aliasing Example

a b c

FIGURE 4.17 Illustration of aliasing on resampled images. (a) A digital image with negligible visual aliasing. (b) Result of resizing the image to 50% of its original size by pixel deletion. Aliasing is clearly visible. (c) Result of blurring the image in (a) with a 3 × 3 averaging filter prior to resizing. The image is slightly more blurred than (b), but aliasing is not longer objectionable. (Original image courtesy of the Signal Compression Laboratory, University of California, Santa Barbara.)

Aliasing Example

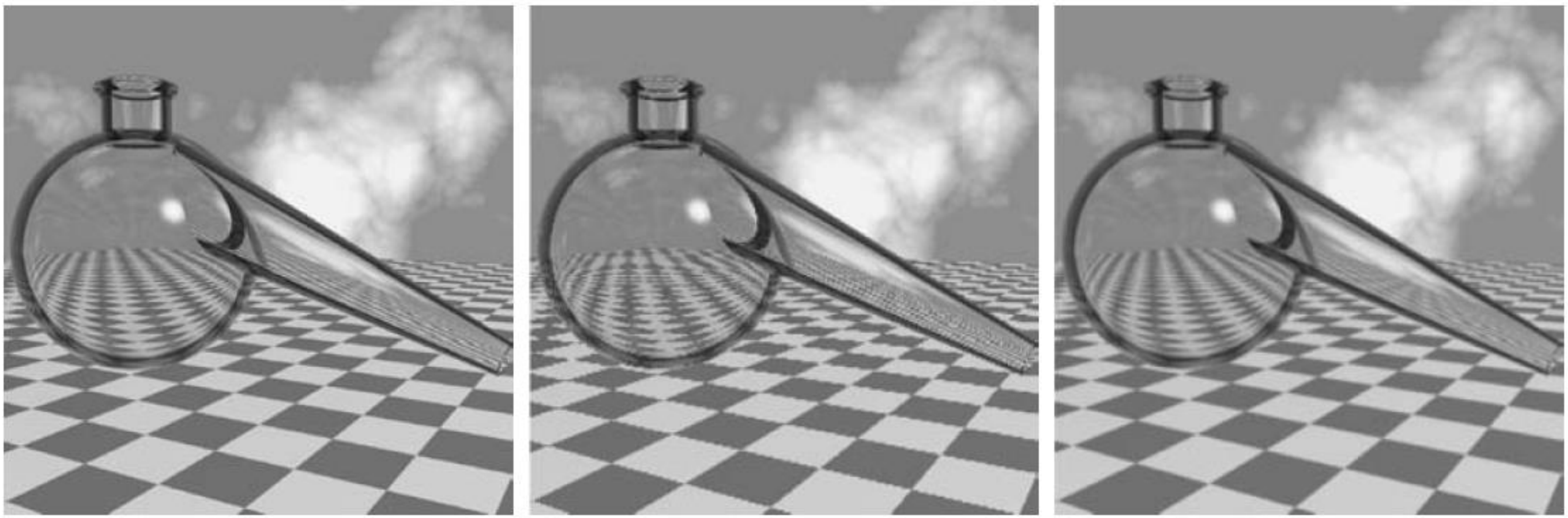

a b c

FIGURE 4.18 Illustration of jaggies. (a) A 1024 × 1024 digital image of a computer-generated scene with negligible visible aliasing. (b) Result of reducing (a) to 25% of its original size using bilinear interpolation. (c) Result of blurring the image in (a) with a 5 × 5 averaging filter prior to resizing it to 25% using bilinear interpolation. (Original image courtesy of D. P. Mitchell, Mental Landscape, LLC.)

2D Discrete Fourier Transform

$$F(u,v) = \sum_{x=0}^{M-1} \sum_{y=0}^{N-1} f(x,y) e^{-j2\pi(\frac{ux}{M}+\frac{vy}{N})}$$

$$f(x,y) = \frac{1}{MN} \sum_{x=0}^{M-1} \sum_{y=0}^{N-1} F(u,v) e^{j2\pi(\frac{ux}{M}+\frac{vy}{N})}$$

$$u, x = 0, 1, \cdots, M$$
$$v, y = 0, 1, \cdots, N$$

Periodicity:

$$F(u,v) = F(u + k_1 M, v + k_2 N)$$
$$f(x,y) = f(x + k_1 M, y + k_2 N)$$

Fourier Spectrum and Phase Angle

$$F(u,v) = |F(u,v)|e^{j\phi(u,v)}$$

spectrum

$$\phi(u,v) = \arctan\frac{I(u,v)}{R(u,v)}$$

phase

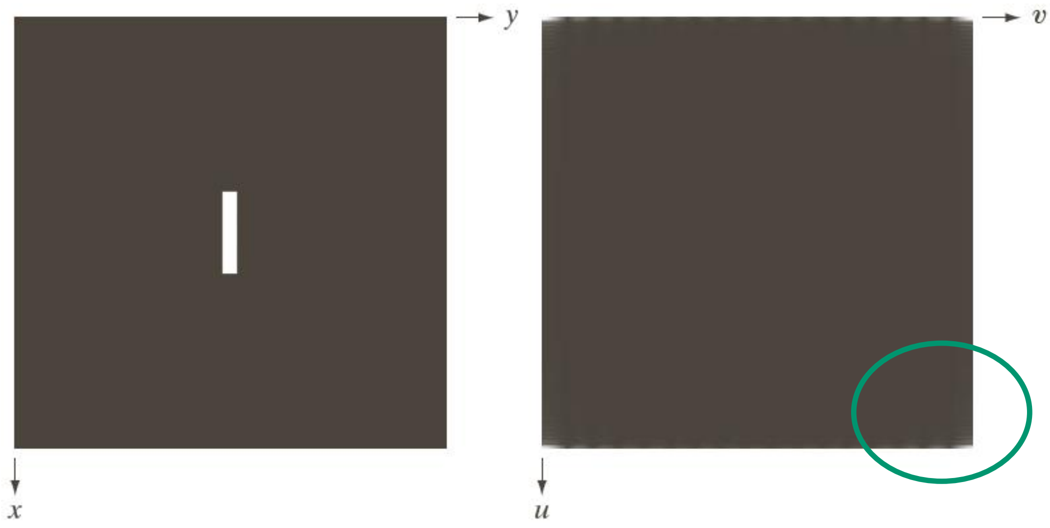

FIGURE 4.24 (a) Image. (b) Spectrum showing bright spots in the four corners.

$$F(0,0) = MN\bar{f}(x,y)$$

Centering the DFT

Modulation/Translation:

$$f(x)e^{j2\pi(u_0 x/M)} \leftrightarrow F(u-u_0)$$

$$f(x)(-1)^x \leftrightarrow F(u-M/2)$$

$$f(x,y)(-1)^{x+y} \leftrightarrow F(u-M/2, v-N/2)$$

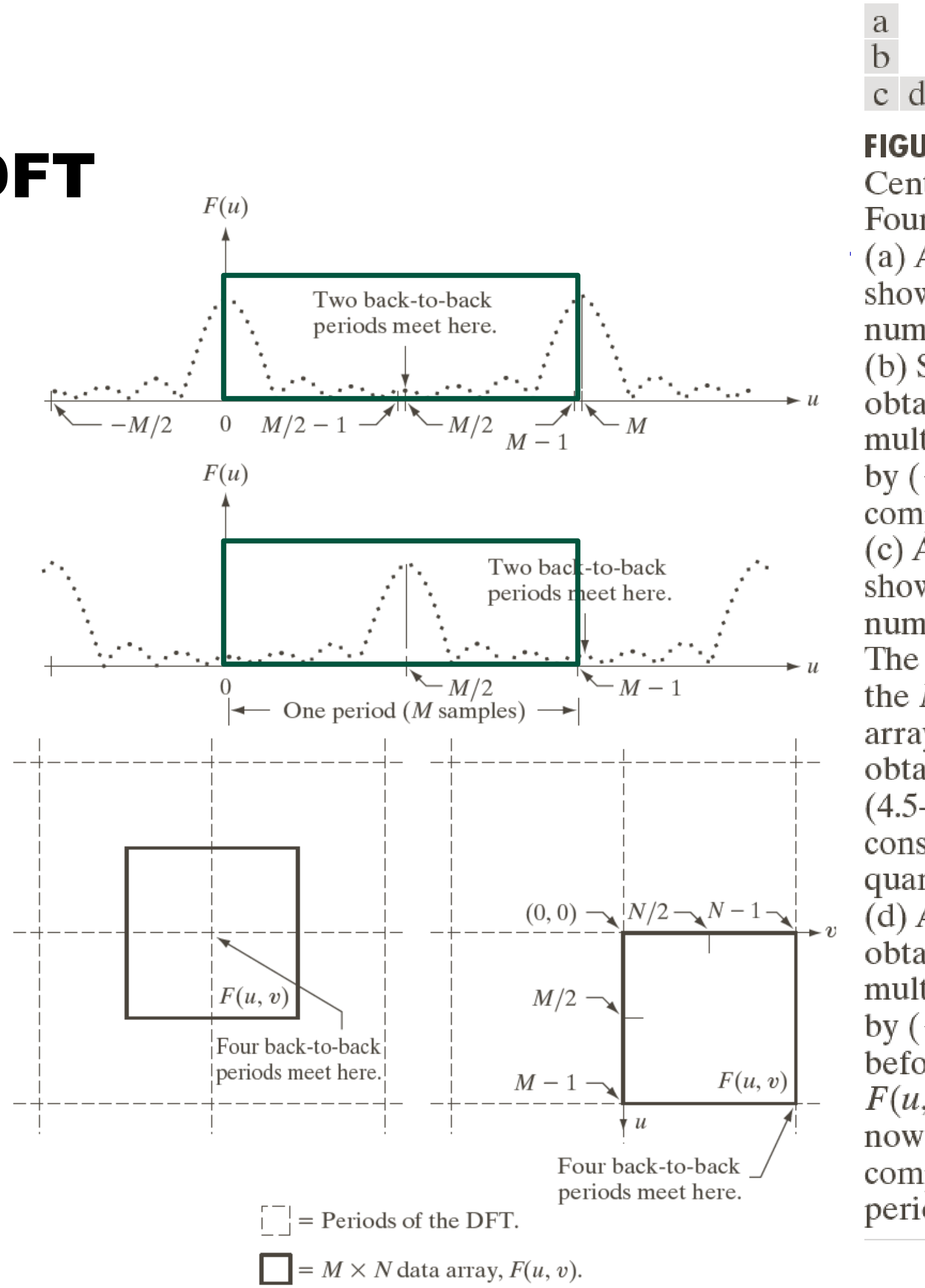

FIGURE 4.23 Centering the Fourier transform. (a) A 1-D DFT showing an infinite number of periods. (b) Shifted DFT obtained by multiplying $f(x)$ by $(-1)^x$ before computing $F(u)$. (c) A 2-D DFT showing an infinite number of periods. The solid area is the $M \times N$ data array, $F(u, v)$, obtained with Eq. (4.5-15). This array consists of four quarter periods. (d) A Shifted DFT obtained by multiplying $f(x, y)$ by $(-1)^{x+y}$ before computing $F(u, v)$. The data now contains one complete, centered period, as in (b).

Fourier Spectrum and Phase Angle

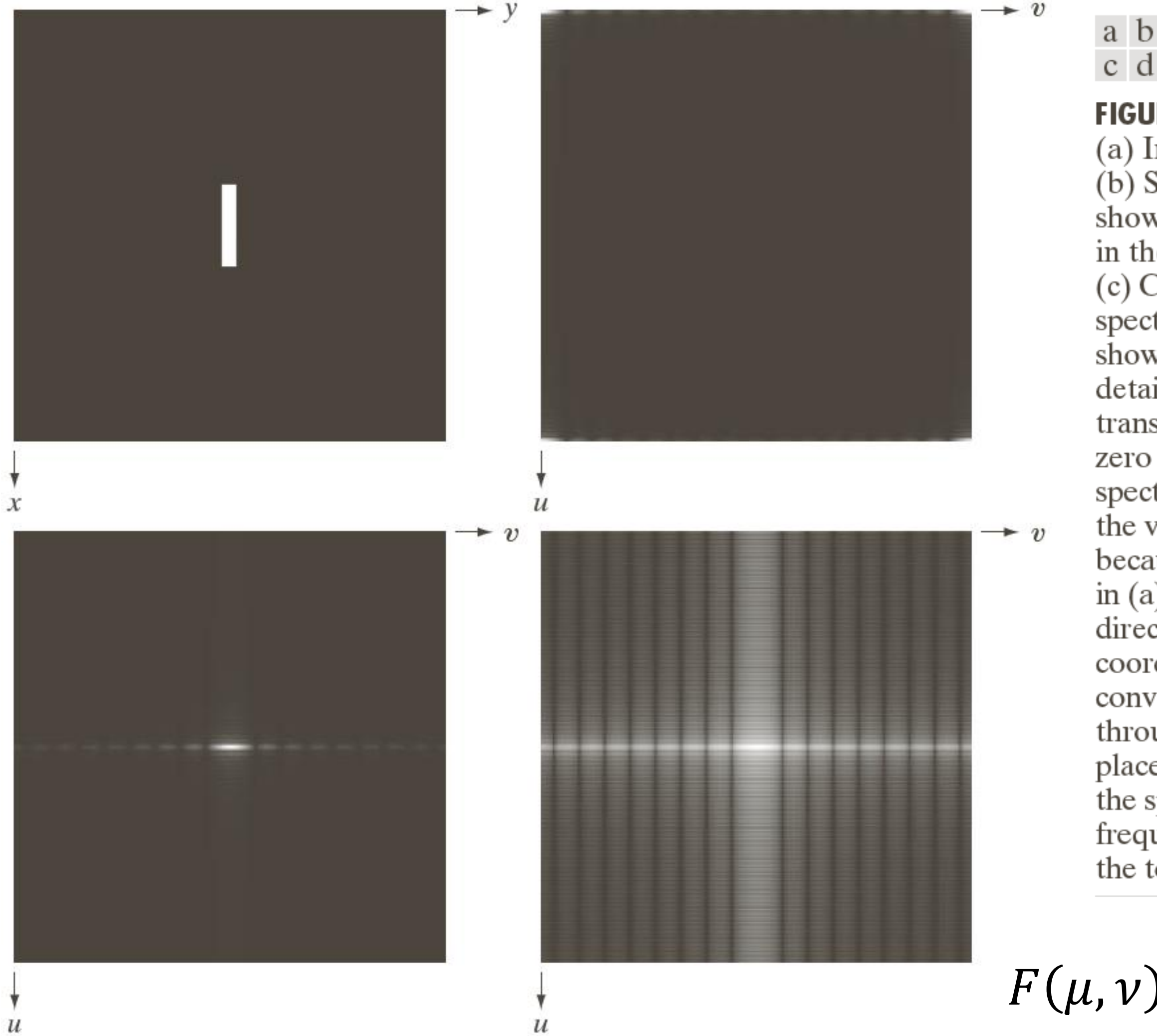

FIGURE 4.24
(a) Image. (b) Spectrum showing bright spots in the four corners. (c) Centered spectrum. (d) Result showing increased detail after a log transformation. The zero crossings of the spectrum are closer in the vertical direction because the rectangle in (a) is longer in that direction. The coordinate convention used throughout the book places the origin of the spatial and frequency domains at the top left.

$$F(\mu,\nu) = ATZ\left[\frac{\sin(\pi\mu T)}{(\pi\mu T)}\right]\left[\frac{\sin(\pi\nu Z)}{(\pi\nu Z)}\right]$$

Fourier Spectrum After Translation and Rotation

$$f(x - x_0, y - y_0) \leftrightarrow$$
$$F(u, v) e^{-j2\pi\left(\frac{ux_0}{M} + \frac{vy_0}{N}\right)}$$
$$\Downarrow$$
$$|F(u, v)|$$

$$f(r, \theta + \theta_0) \leftrightarrow$$
$$F(w, \varphi + \theta_0)$$
$$x = r\cos\theta, y = r\sin\theta$$
$$u = w\cos\varphi, v = w\sin\varphi$$

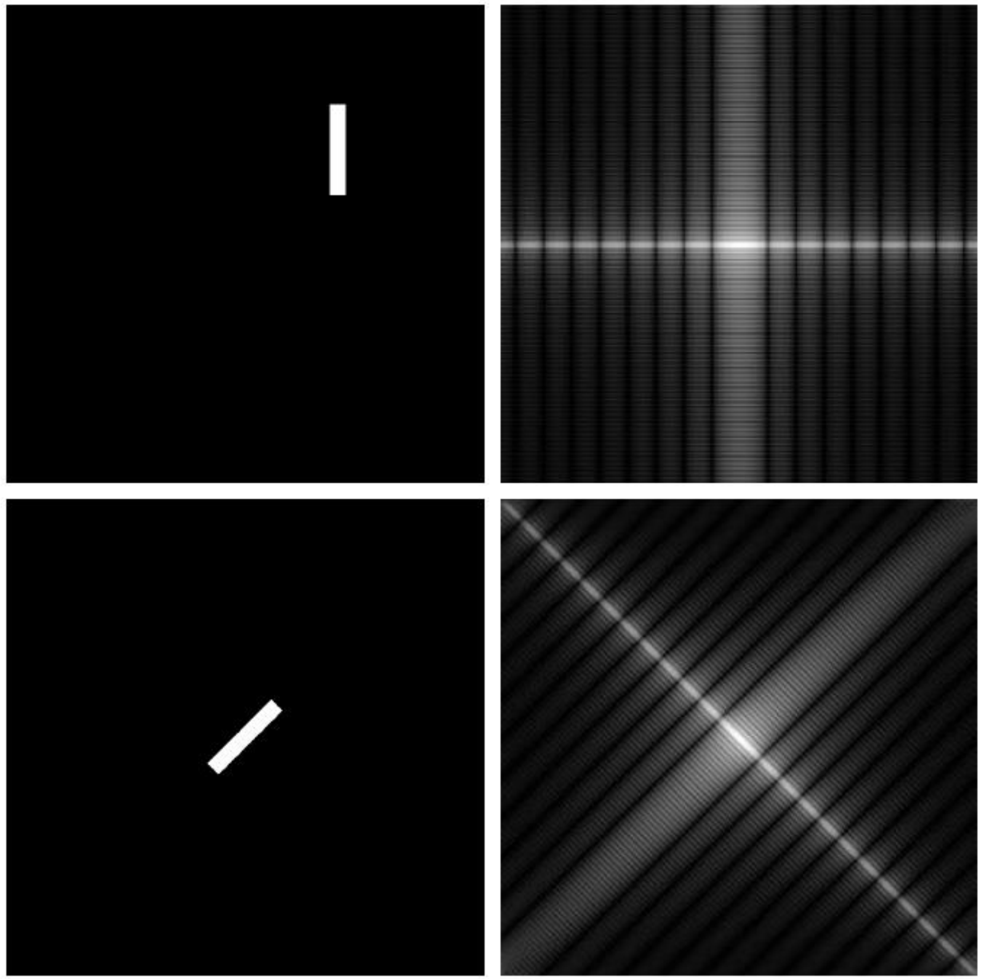

| a | b |
| c | d |

FIGURE 4.25 (a) The rectangle in Fig. 4.24(a) translated, and (b) the corresponding spectrum. (c) Rotated rectangle, and (d) the corresponding spectrum. The spectrum corresponding to the translated rectangle is identical to the spectrum corresponding to the original image in Fig. 4.24(a).

The Roles of Fourier Spectrum and Phase Angle

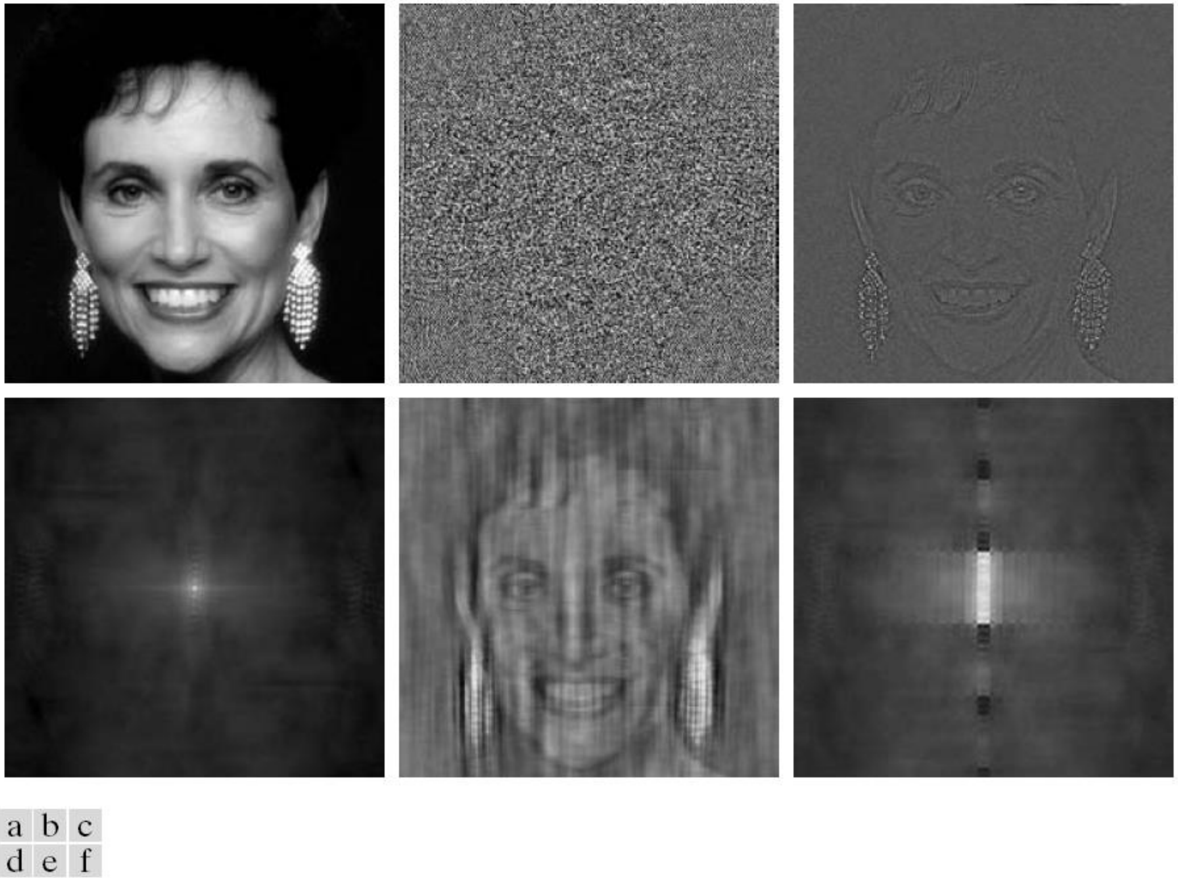

FIGURE 4.27 (a) Woman. (b) Phase angle. (c) Woman reconstructed using only the phase angle. (d) Woman reconstructed using only the spectrum. (e) Reconstruction using the phase angle corresponding to the woman and the spectrum corresponding to the rectangle in Fig. 4.24(a). (f) Reconstruction using the phase of the rectangle and the spectrum of the woman.

2D Convolution Theorem (Zero Padding)

Length for the input signals after zero-padding

$$P \geq A + B - 1$$

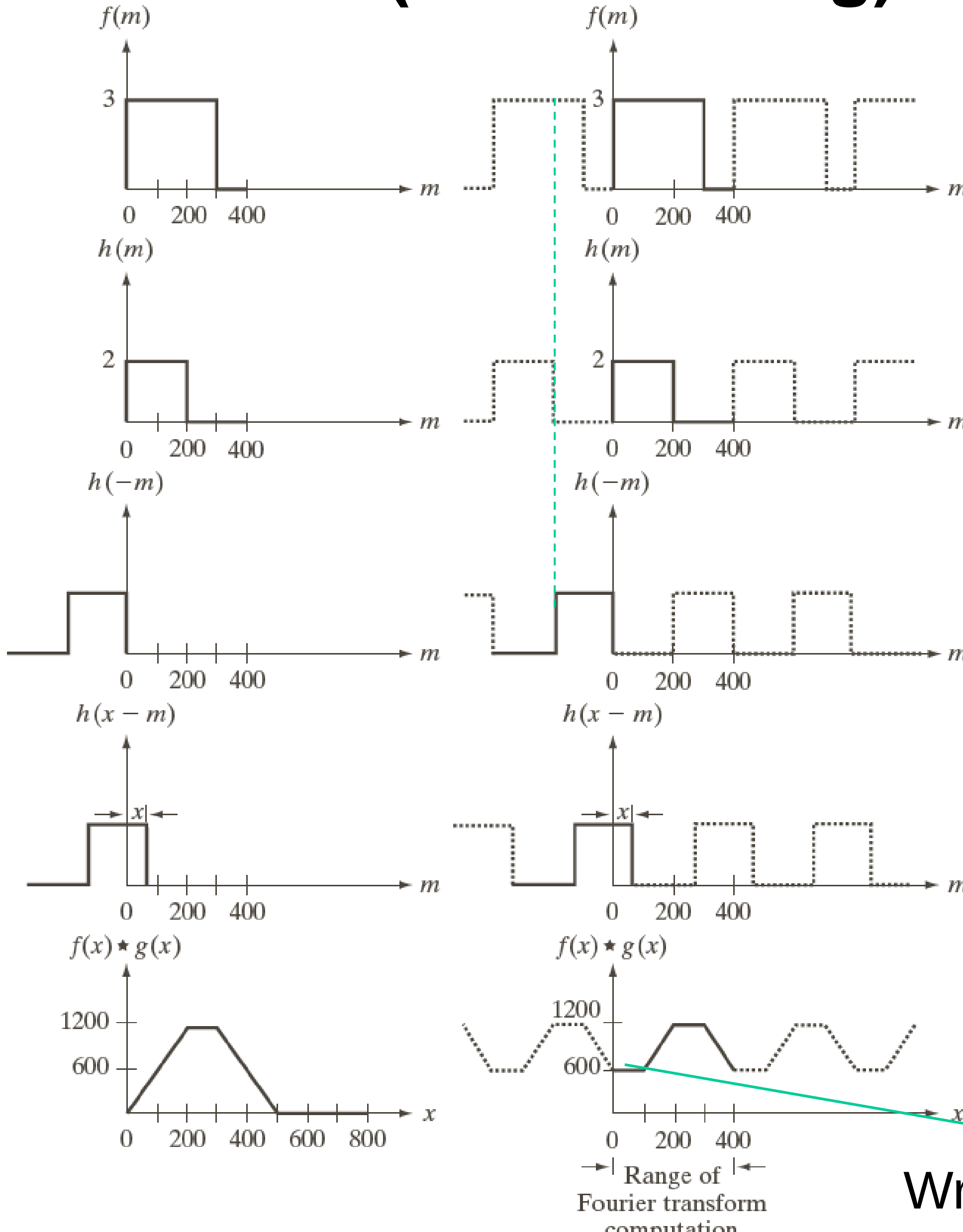

a f
b g
c h
d i
e j

FIGURE 4.28 Left column: convolution of two discrete functions obtained using the approach discussed in Section 3.4.2. The result in (e) is correct. Right column: Convolution of the same functions, but taking into account the periodicity implied by the DFT. Note in (j) how data from adjacent periods produce wraparound error, yielding an incorrect convolution result. To obtain the correct result, function padding must be used.

Wraparound error

2D DFT Properties

Name	Expression(s)
1) Discrete Fourier transform (DFT) of $f(x, y)$	$F(u, v) = \sum_{x=0}^{M-1} \sum_{y=0}^{N-1} f(x, y) e^{-j2\pi(ux/M + vy/N)}$
2) Inverse discrete Fourier transform (IDFT) of $F(u, v)$	$f(x, y) = \frac{1}{MN} \sum_{u=0}^{M-1} \sum_{v=0}^{N-1} F(u, v) e^{j2\pi(ux/M + vy/N)}$
3) Polar representation	$F(u, v) = \lvert F(u, v)\rvert e^{j\phi(u,v)}$
4) Spectrum	$\lvert F(u, v)\rvert = \left[R^2(u, v) + I^2(u, v)\right]^{1/2}$ $R = \text{Real}(F);\quad I = \text{Imag}(F)$
5) Phase angle	$\phi(u, v) = \tan^{-1}\left[\frac{I(u, v)}{R(u, v)}\right]$
6) Power spectrum	$P(u, v) = \lvert F(u, v)\rvert^2$
7) Average value	$\overline{f}(x, y) = \frac{1}{MN} \sum_{x=0}^{M-1} \sum_{y=0}^{N-1} f(x, y) = \frac{1}{MN} F(0, 0)$

(Continued)

TABLE 4.2 Summary of DFT definitions and corresponding expressions.

2D DFT Properties (cont.)

Name	Expression(s)
8) Periodicity (k_1 and k_2 are integers)	$F(u, v) = F(u + k_1M, v) = F(u, v + k_2N) = F(u + k_1M, v + k_2N)$ $f(x, y) = f(x + k_1M, y) = f(x, y + k_2N) = f(x + k_1M, y + k_2N)$
9) Convolution	$f(x, y) \bigstar h(x, y) = \sum_{m=0}^{M-1} \sum_{n=0}^{N-1} f(m, n)h(x - m, y - n)$
10) Correlation	$f(x, y) \star h(x, y) = \sum_{m=0}^{M-1} \sum_{n=0}^{N-1} f^*(m, n)h(x + m, y + n)$
11) Separability	The 2-D DFT can be computed by computing 1-D DFT transforms along the rows (columns) of the image, followed by 1-D transforms along the columns (rows) of the result. See Section 4.11.1.
12) Obtaining the inverse Fourier transform using a forward transform algorithm.	$MNf^*(x, y) = \sum_{u=0}^{M-1} \sum_{v=0}^{N-1} F^*(u, v)e^{-j2\pi(ux/M + vy/N)}$ This equation indicates that inputting $F^*(u, v)$ into an algorithm that computes the forward transform (right side of above equation) yields $MNf^*(x, y)$. Taking the complex conjugate and dividing by MN gives the desired inverse. See Section 4.11.2.

TABLE 4.2
(Continued)

2D DFT Properties (Symmetry)

	Spatial Domain†		Frequency Domain†
1)	$f(x, y)$ real	$\Leftrightarrow$	$F^*(u, v) = F(-u, -v)$
2)	$f(x, y)$ imaginary	$\Leftrightarrow$	$F^*(-u, -v) = -F(u, v)$
3)	$f(x, y)$ real	$\Leftrightarrow$	$R(u, v)$ even; $I(u, v)$ odd
4)	$f(x, y)$ imaginary	$\Leftrightarrow$	$R(u, v)$ odd; $I(u, v)$ even
5)	$f(-x, -y)$ real	$\Leftrightarrow$	$F^*(u, v)$ complex
6)	$f(-x, -y)$ complex	$\Leftrightarrow$	$F(-u, -v)$ complex
7)	$f^*(x, y)$ complex	$\Leftrightarrow$	$F^*(-u - v)$ complex
8)	$f(x, y)$ real and even	$\Leftrightarrow$	$F(u, v)$ real and even
9)	$f(x, y)$ real and odd	$\Leftrightarrow$	$F(u, v)$ imaginary and odd
10)	$f(x, y)$ imaginary and even	$\Leftrightarrow$	$F(u, v)$ imaginary and even
11)	$f(x, y)$ imaginary and odd	$\Leftrightarrow$	$F(u, v)$ real and odd
12)	$f(x, y)$ complex and even	$\Leftrightarrow$	$F(u, v)$ complex and even
13)	$f(x, y)$ complex and odd	$\Leftrightarrow$	$F(u, v)$ complex and odd

†Recall that x, y, u, and v are *discrete* (integer) variables, with x and u in the range $[0, M - 1]$, and y, and v in the range $[0, N - 1]$. To say that a complex function is *even* means that its real *and* imaginary parts are even, and similarly for an odd complex function.

TABLE 4.1 Some symmetry properties of the 2-D DFT and its inverse. $R(u, v)$ and $I(u, v)$ are the real and imaginary parts of $F(u, v)$, respectively. The term *complex* indicates that a function has nonzero real and imaginary parts.

Even (symmetric): $w_e(x, y) = w_e(M - x, N - y)$

Odd (antisymmetric): $w_o(x, y) = -w_o(M - x, N - y)$

2D DFT Properties (cont.)

Name	DFT Pairs
1) Symmetry properties	See Table 4.1
2) Linearity	$af_1(x, y) + bf_2(x, y) \Leftrightarrow aF_1(u, v) + bF_2(u, v)$
3) Translation (general)	$f(x, y)e^{j2\pi(u_0x/M + v_0y/N)} \Leftrightarrow F(u - u_0, v - v_0)$ $f(x - x_0, y - y_0) \Leftrightarrow F(u, v)e^{-j2\pi(ux_0/M + vy_0/N)}$
4) Translation to center of the frequency rectangle, $(M/2, N/2)$	$f(x, y)(-1)^{x+y} \Leftrightarrow F(u - M/2, v - N/2)$ $f(x - M/2, y - N/2) \Leftrightarrow F(u, v)(-1)^{u+v}$
5) Rotation	$f(r, \theta + \theta_0) \Leftrightarrow F(\omega, \varphi + \theta_0)$ $x = r\cos\theta \quad y = r\sin\theta \quad u = \omega\cos\varphi \quad v = \omega\sin\varphi$
6) Convolution theorem[†]	$f(x, y) \star h(x, y) \Leftrightarrow F(u, v)H(u, v)$ $f(x, y)h(x, y) \Leftrightarrow F(u, v) \star H(u, v)$

(*Continued*)

TABLE 4.3
Summary of DFT pairs. The closed-form expressions in 12 and 13 are valid only for continuous variables. They can be used with discrete variables by sampling the closed-form, continuous expressions.

2D DFT Properties (cont.)

Name	DFT Pairs
7) Correlation theorem†	$f(x, y) \star h(x, y) \Leftrightarrow F^*(u, v)\, H(u, v)$ $f^*(x, y)h(x, y) \Leftrightarrow F(u, v) \star H(u, v)$
8) Discrete unit impulse	$\delta(x, y) \Leftrightarrow 1$
9) Rectangle	$\text{rect}[a, b] \Leftrightarrow ab\dfrac{\sin(\pi ua)}{(\pi ua)}\dfrac{\sin(\pi vb)}{(\pi vb)}e^{-j\pi(ua+vb)}$
10) Sine	$\sin(2\pi u_0 x + 2\pi v_0 y) \Leftrightarrow$ $j\dfrac{1}{2}\left[\delta(u + Mu_0, v + Nv_0) - \delta(u - Mu_0, v - Nv_0)\right]$
11) Cosine	$\cos(2\pi u_0 x + 2\pi v_0 y) \Leftrightarrow$ $\dfrac{1}{2}\left[\delta(u + Mu_0, v + Nv_0) + \delta(u - Mu_0, v - Nv_0)\right]$
The following Fourier transform pairs are derivable only for continuous variables, denoted as before by t and z for spatial variables and by μ and ν for frequency variables. These results can be used for DFT work by sampling the continuous forms.	
12) *Differentiation* (The expressions on the right assume that $f(\pm\infty, \pm\infty) = 0$.)	$\left(\dfrac{\partial}{\partial t}\right)^m\left(\dfrac{\partial}{\partial z}\right)^n f(t, z) \Leftrightarrow (j2\pi\mu)^m(j2\pi\nu)^n F(\mu, \nu)$ $\dfrac{\partial^m f(t, z)}{\partial t^m} \Leftrightarrow (j2\pi\mu)^m F(\mu, \nu); \dfrac{\partial^n f(t, z)}{\partial z^n} \Leftrightarrow (j2\pi\nu)^n F(\mu, \nu)$
13) *Gaussian*	$A2\pi\sigma^2 e^{-2\pi^2\sigma^2(t^2+z^2)} \Leftrightarrow Ae^{-(\mu^2+\nu^2)/2\sigma^2}$ (A is a constant)

†Assumes that the functions have been extended by zero padding. Convolution and correlation are associative, commutative, and distributive.

TABLE 4.3
(*Continued*)

Basics of Filtering in Frequency Domain

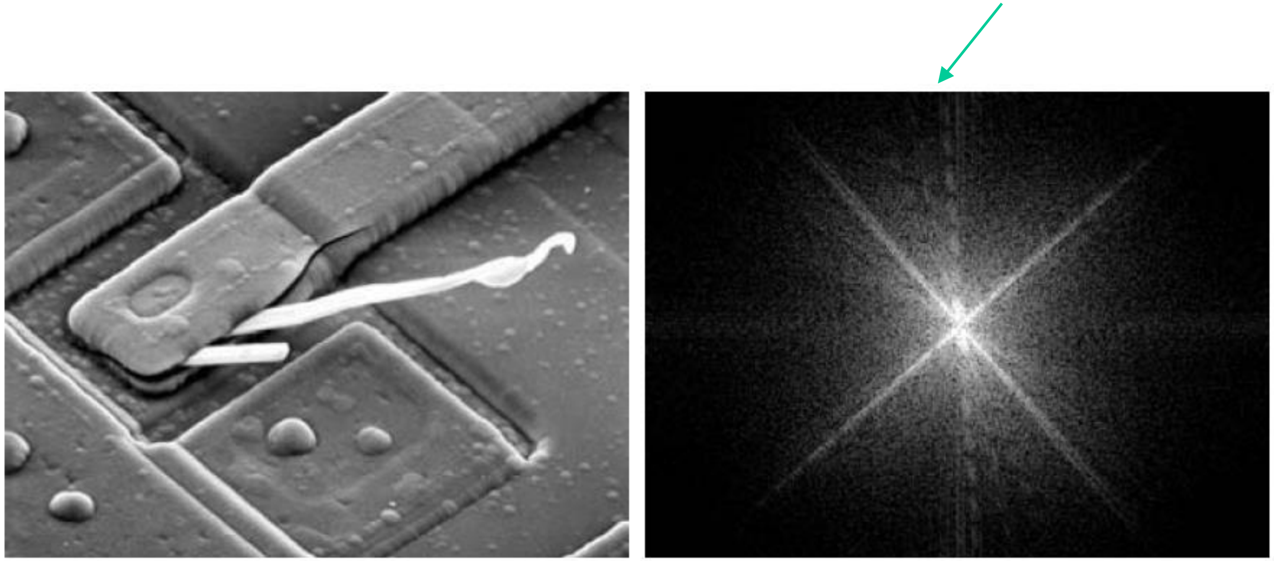

a b

FIGURE 4.29 (a) SEM image of a damaged integrated circuit. (b) Fourier spectrum of (a). (Original image courtesy of Dr. J. M. Hudak, Brockhouse Institute for Materials Research, McMaster University, Hamilton, Ontario, Canada.)

Frequency Domain Filtering Fundamentals

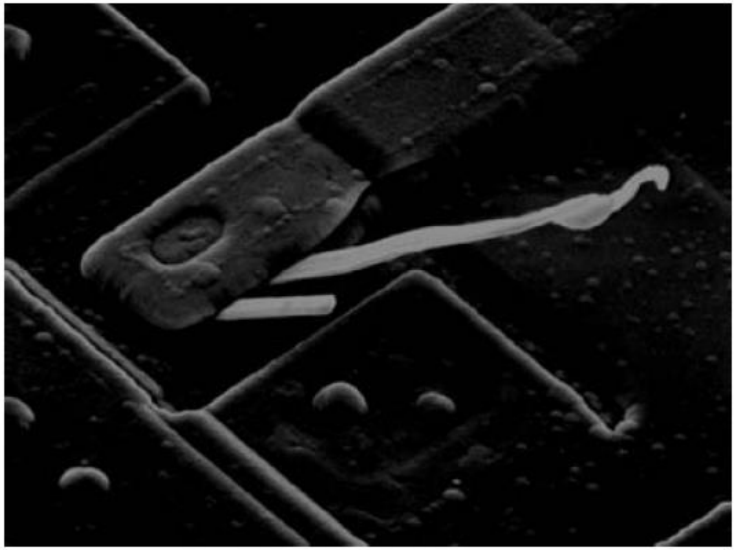

FIGURE 4.30 Result of filtering the image in Fig. 4.29(a) by setting to 0 the term $F(M/2, N/2)$ in the Fourier transform.

$$g(x,y) \leftrightarrow H(u,v)F(u,v)$$

Centered $F(M/2, N/2) = MN\bar{f}(x,y)$ → **dc term**

Low-Pass and High-Pass Filters

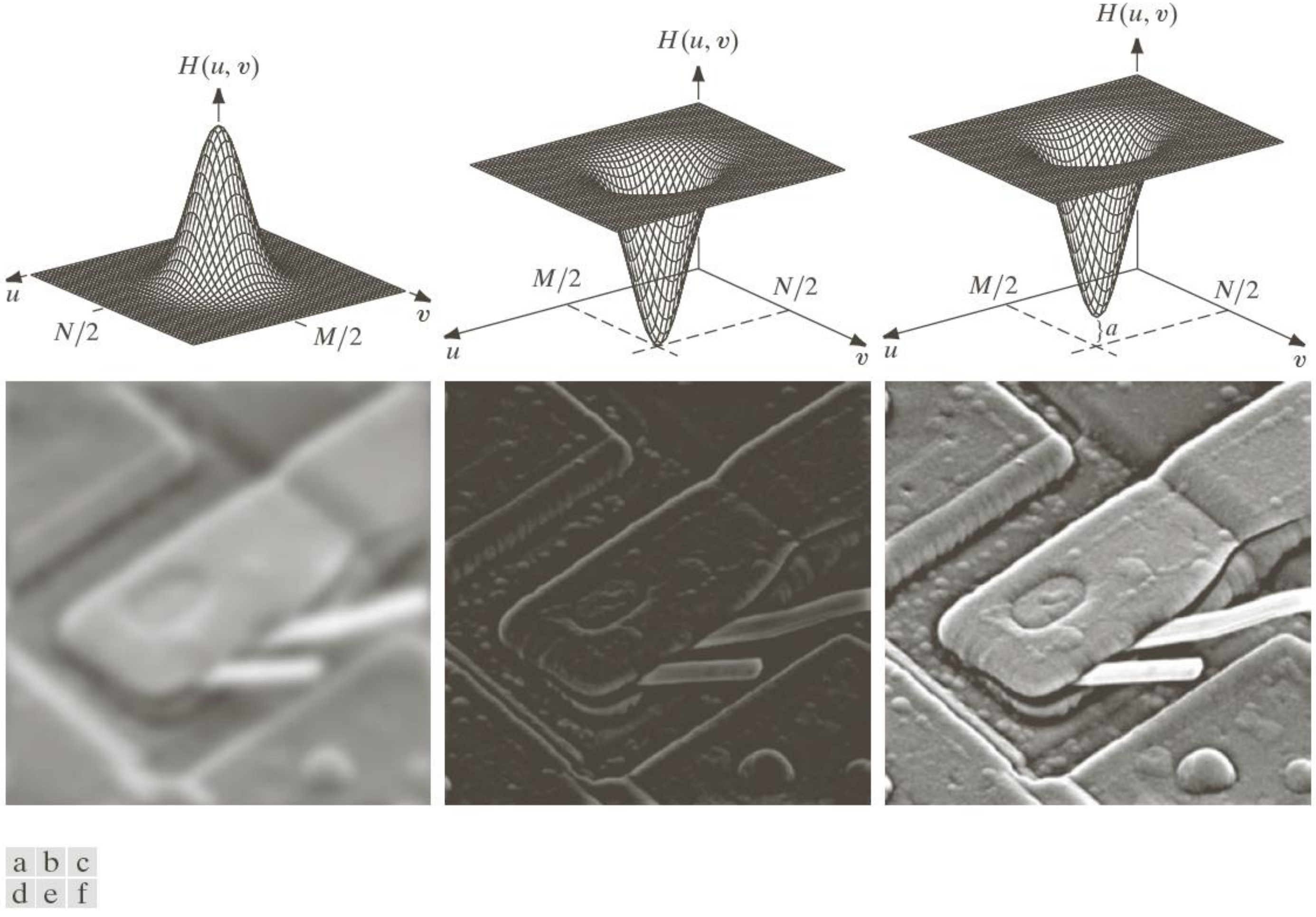

FIGURE 4.31 Top row: frequency domain filters. Bottom row: corresponding filtered images obtained using Eq. (4.7-1). We used $a = 0.85$ in (c) to obtain (f) (the height of the filter itself is 1). Compare (f) with Fig. 4.29(a).

Effects of Zero-Padding

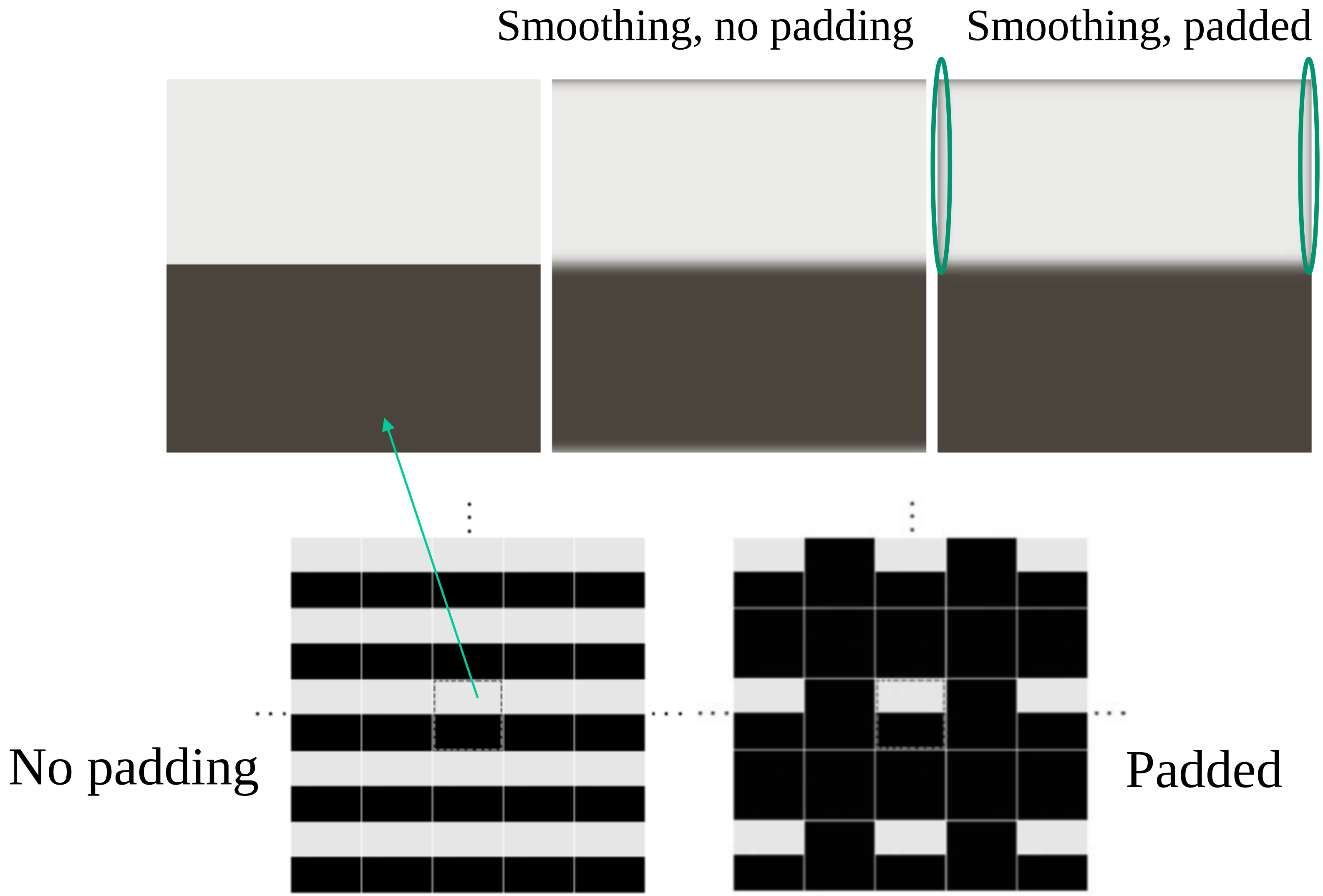

Spatial Zero-Padding for the Filter

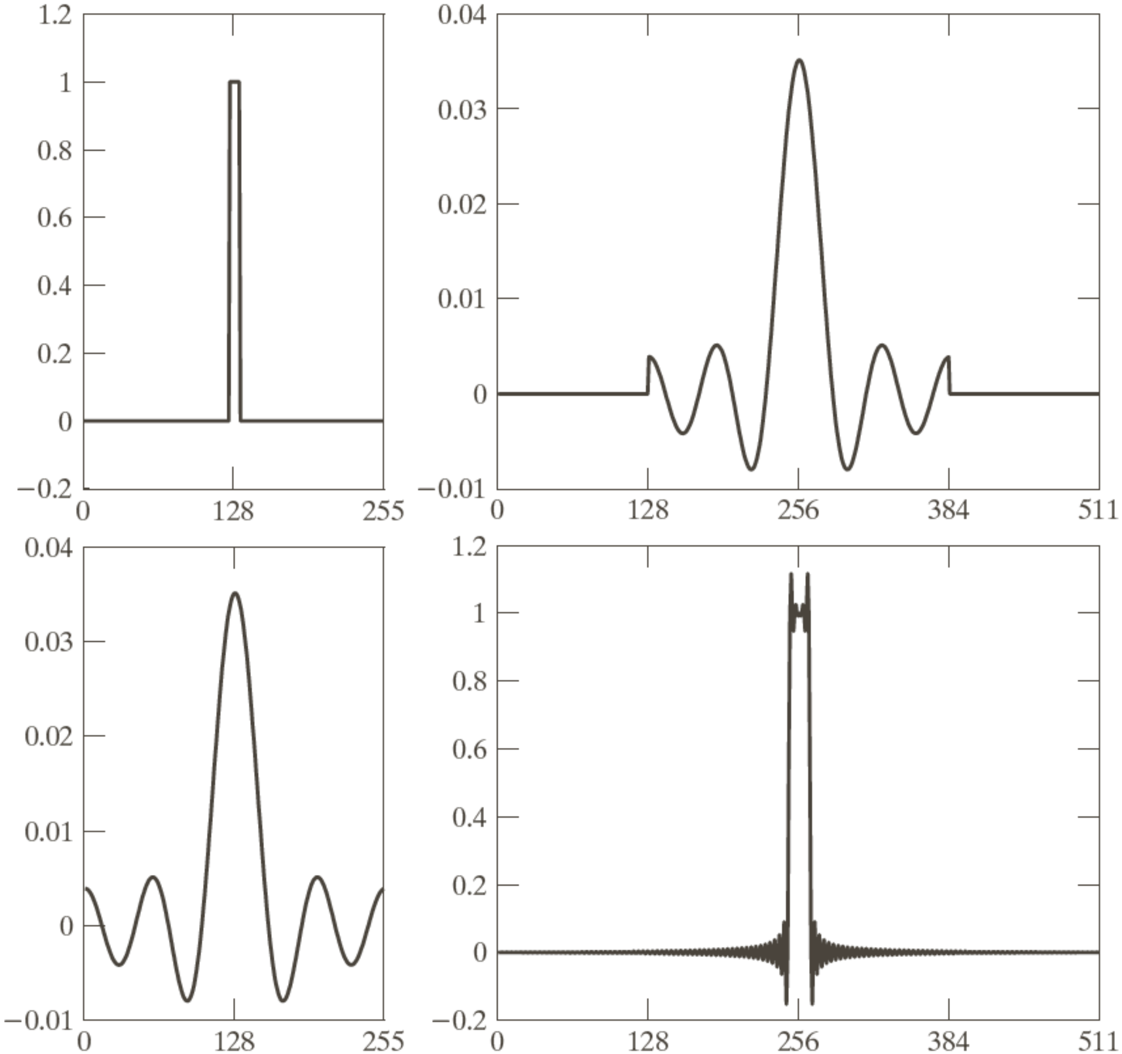

a	c
b	d

FIGURE 4.34
(a) Original filter specified in the (centered) frequency domain. (b) Spatial representation obtained by computing the IDFT of (a). (c) Result of padding (b) to twice its length (note the discontinuities). (d) Corresponding filter in the frequency domain obtained by computing the DFT of (c). Note the ringing caused by the discontinuities in (c). (The curves appear continuous because the points were joined to simplify visual analysis.)

Summary: Filtering in the Frequency Domain

1. For $f(x, y)$, find $P = 2M$, $Q = 2N$

2. Form a padded image $f_p(x, y)$

3. Centering: Multiply $f_p(x, y)$ by $(-1)^{x+y}$

4. Compute DFT $F(u, v)$

5. Generate a real symmetric filter $H(u, v)$ of a size $P \times Q$, centered at $(P/2, Q/2)$ and make $G(u, v) = H(u, v)F(u, v)$

6. Obtain the processed image (should be real in theory)

$$g_p(x, y) = \{\text{real}[g(x, y)]\}(-1)^{x+y}$$

7. Obtained the final processed results $g(x, y)$ from the top left $M \times N$ region

An Example

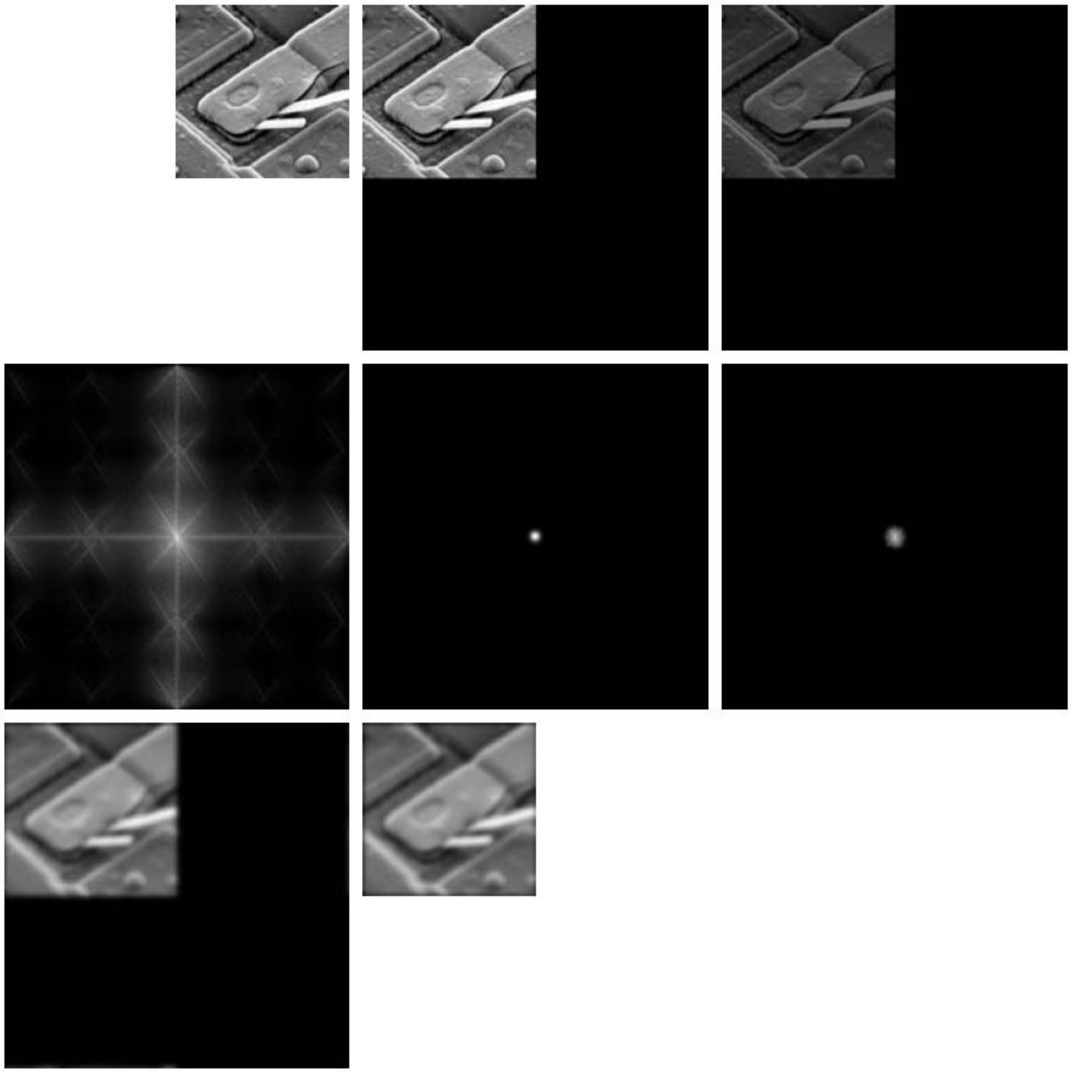

a	b	c
d	e	f
g	h	

FIGURE 4.36
(a) An $M \times N$ image, f.
(b) Padded image, f_p of size $P \times Q$.
(c) Result of multiplying f_p by $(-1)^{x+y}$.
(d) Spectrum of F_p. (e) Centered Gaussian lowpass filter, H, of size $P \times Q$.
(f) Spectrum of the product HF_p.
(g) g_p, the product of $(-1)^{x+y}$ and the real part of the IDFT of HF_p.
(h) Final result, g, obtained by cropping the first M rows and N columns of g_p.

Correspondence to the Spatial Domain Filter

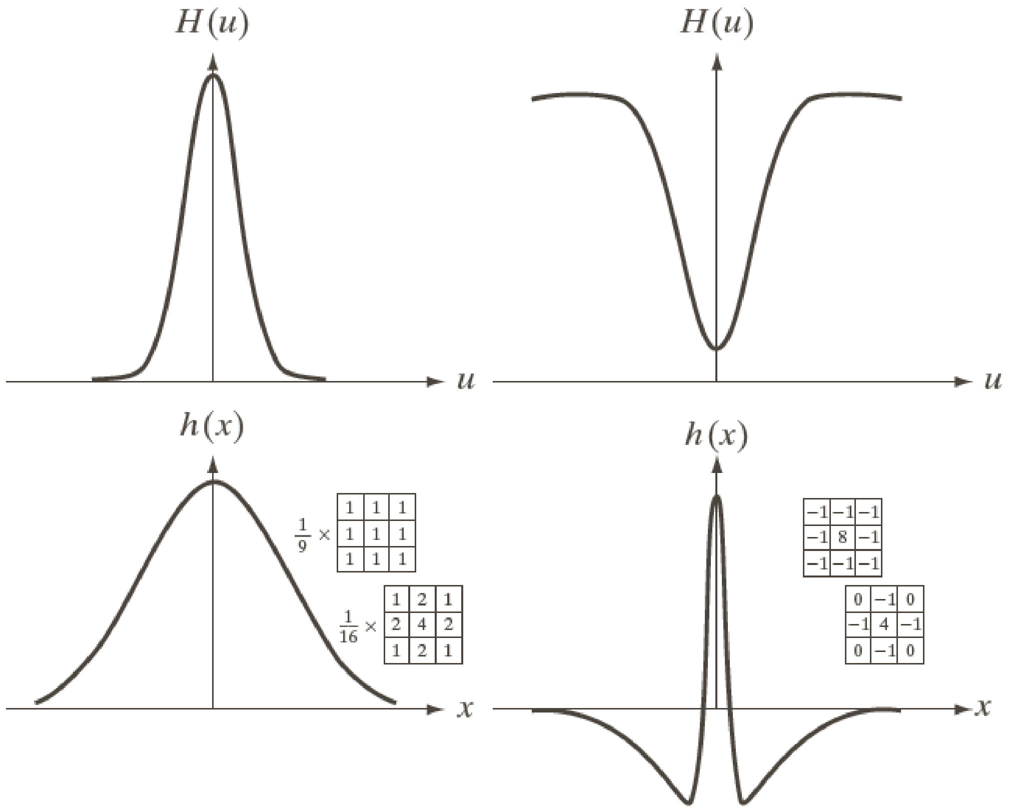

a c
b d

FIGURE 4.37 (a) A 1-D Gaussian lowpass filter in the frequency domain. (b) Spatial lowpass filter corresponding to (a). (c) Gaussian highpass filter in the frequency domain. (d) Spatial highpass filter corresponding to (c). The small 2-D masks shown are spatial filters we used in Chapter 3.

The FT of a Gaussian function is still a Gaussian function

An Example (Sobel Mask)

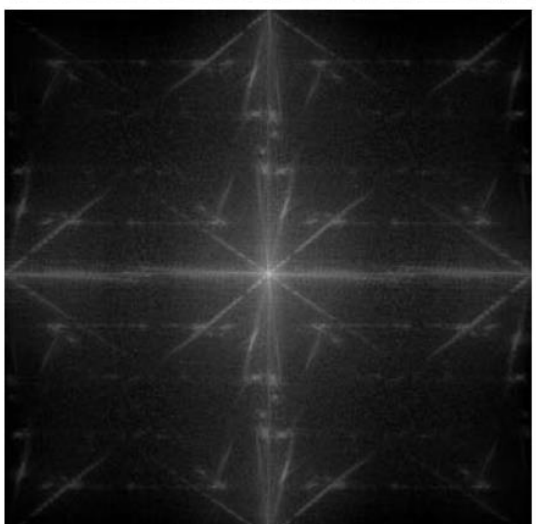

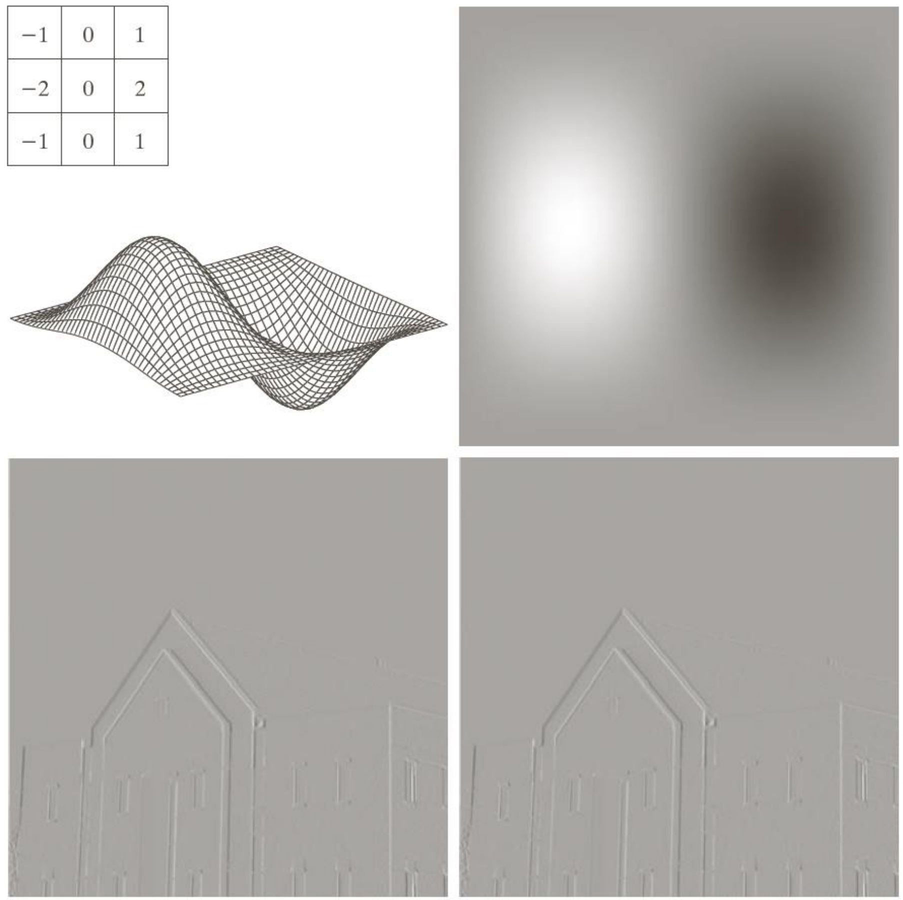

a b
c d

FIGURE 4.39 (a) A spatial mask and perspective plot of its corresponding frequency domain filter. (b) Filter shown as an image. (c) Result of filtering Fig. 4.38(a) in the frequency domain with the filter in (b). (d) Result of filtering the same image with the spatial filter in (a). The results are identical.

Image Smoothing Using Frequency Domain Filters – Ideal Lowpass Filter

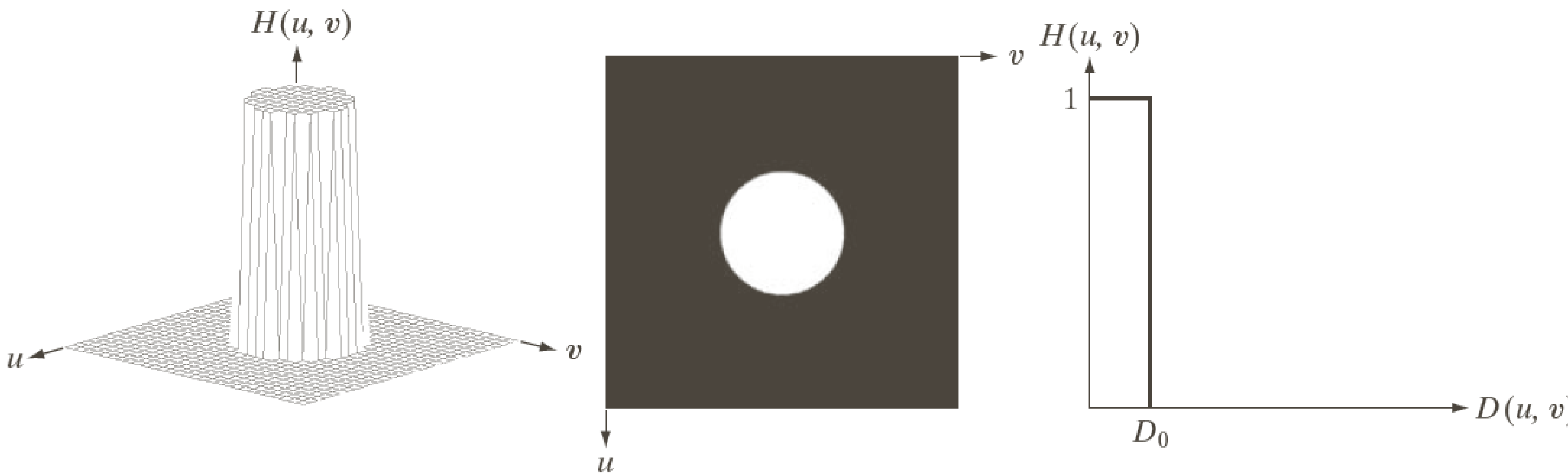

a b c

FIGURE 4.40 (a) Perspective plot of an ideal lowpass-filter transfer function. (b) Filter displayed as an image. (c) Filter radial cross section.

Locating the Cut-Off Frequency

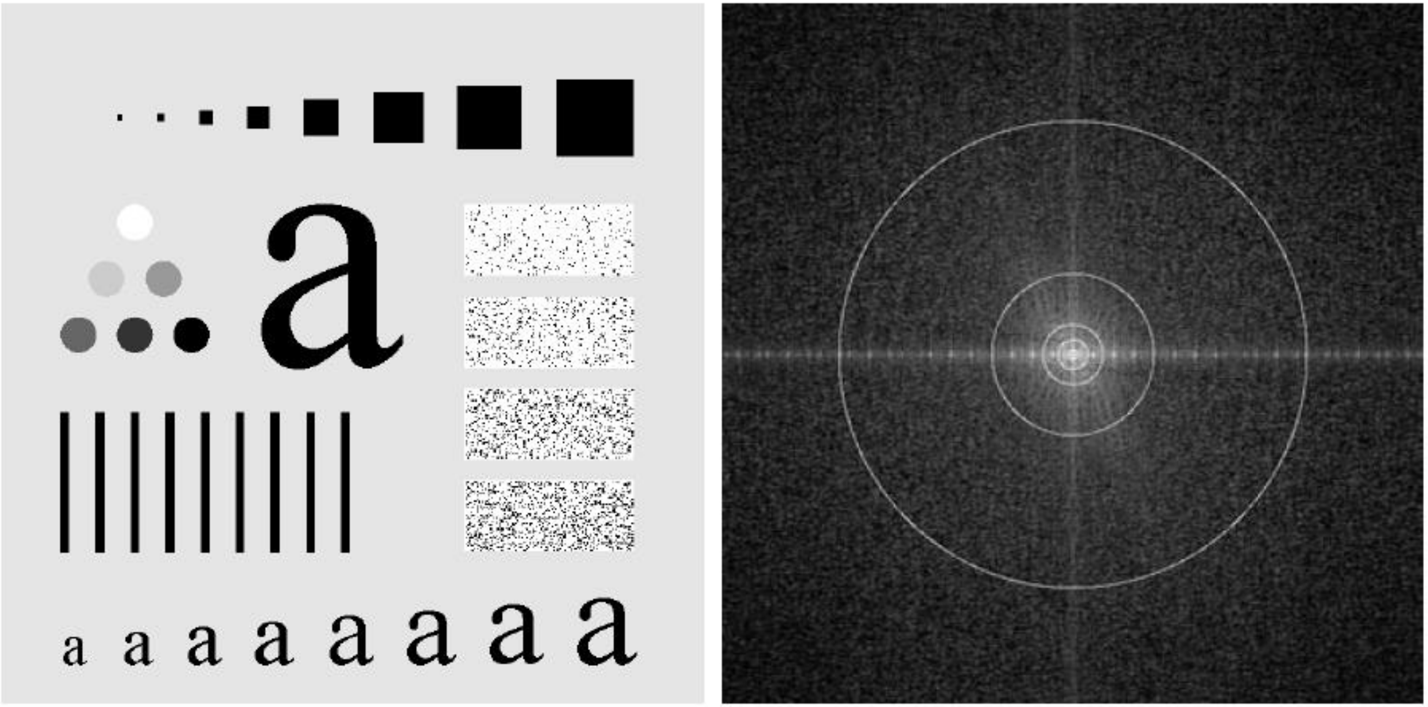

a b

FIGURE 4.41 (a) Test pattern of size 688 × 688 pixels, and (b) its Fourier spectrum. The spectrum is double the image size due to padding but is shown in half size so that it fits in the page. The superimposed circles have radii equal to 10, 30, 60, 160, and 460 with respect to the full-size spectrum image. These radii enclose 87.0, 93.1, 95.7, 97.8, and 99.2% of the padded image power, respectively.

Applying the ILPF – Blurring and Ringing

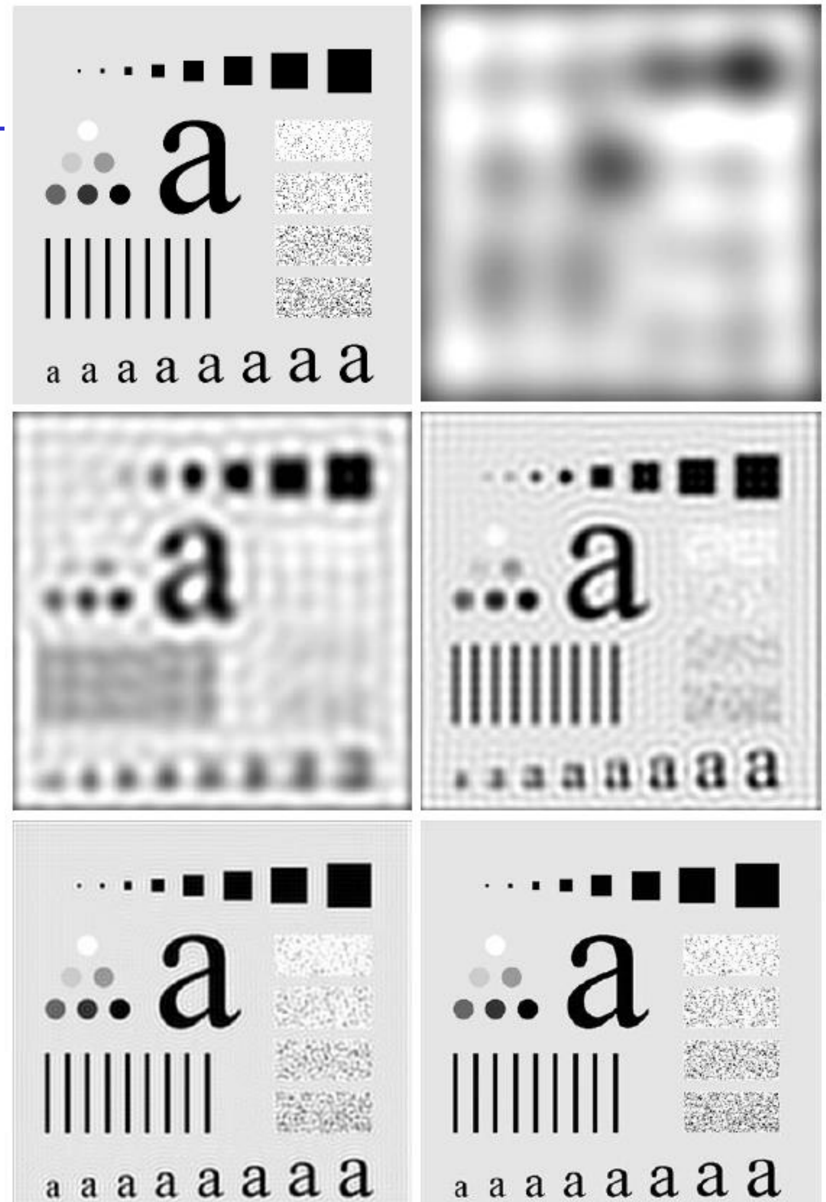

Original

ILPF, cutoff 10,
Energy 87%

ILPF, cutoff 30
Energy 93.1%

ILPF, cutoff 60
Energy 95.7%

ILPF, cutoff 160
Energy 97.8%

ILPF, cutoff 460
Energy 99.2%

Why?

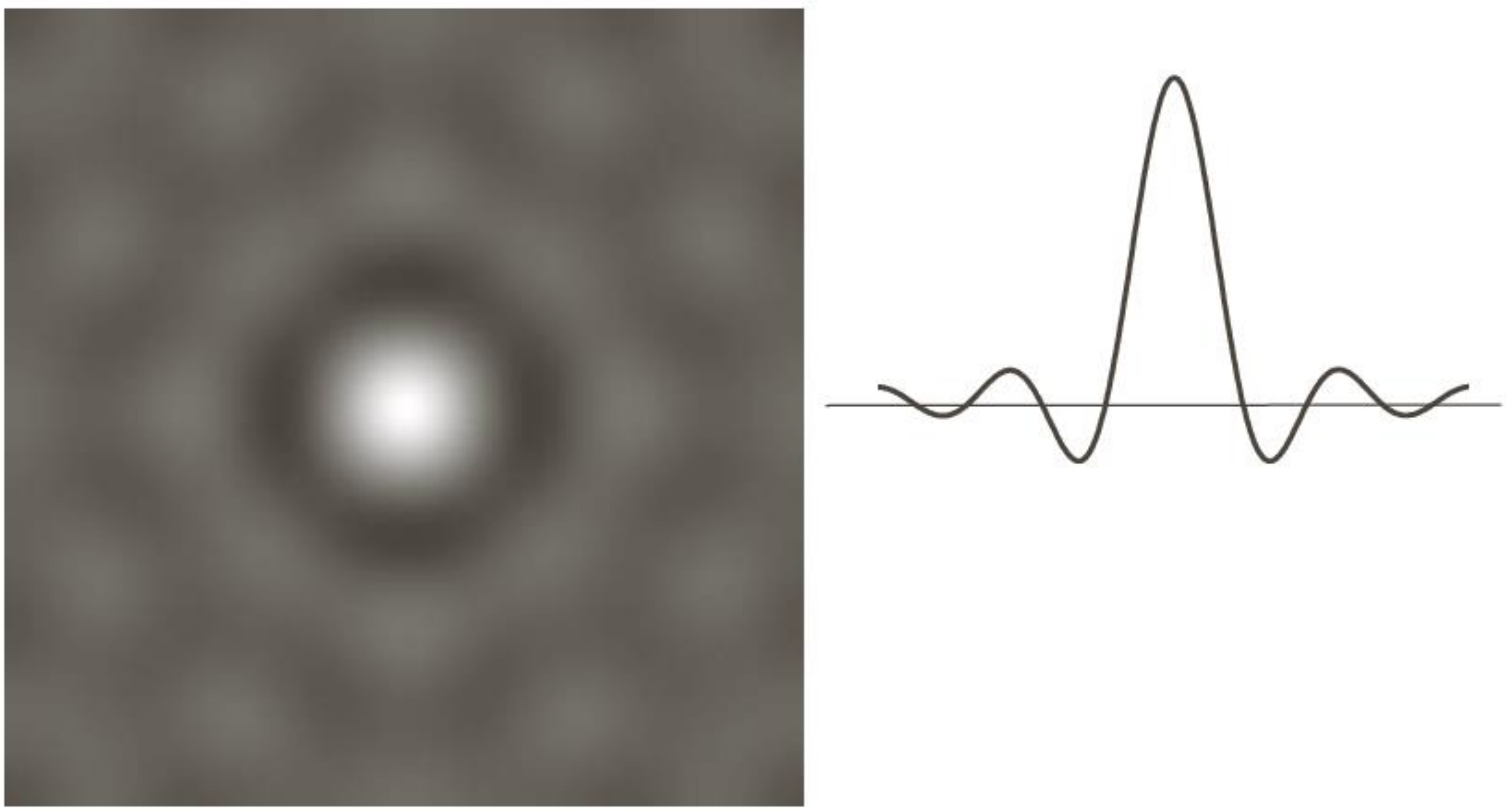

a b

FIGURE 4.43 (a) Representation in the spatial domain of an ILPF of radius 5 and size 1000 × 1000. (b) Intensity profile of a horizontal line passing through the center of the image.

Butterworth Lowpass Filters (BLPF)

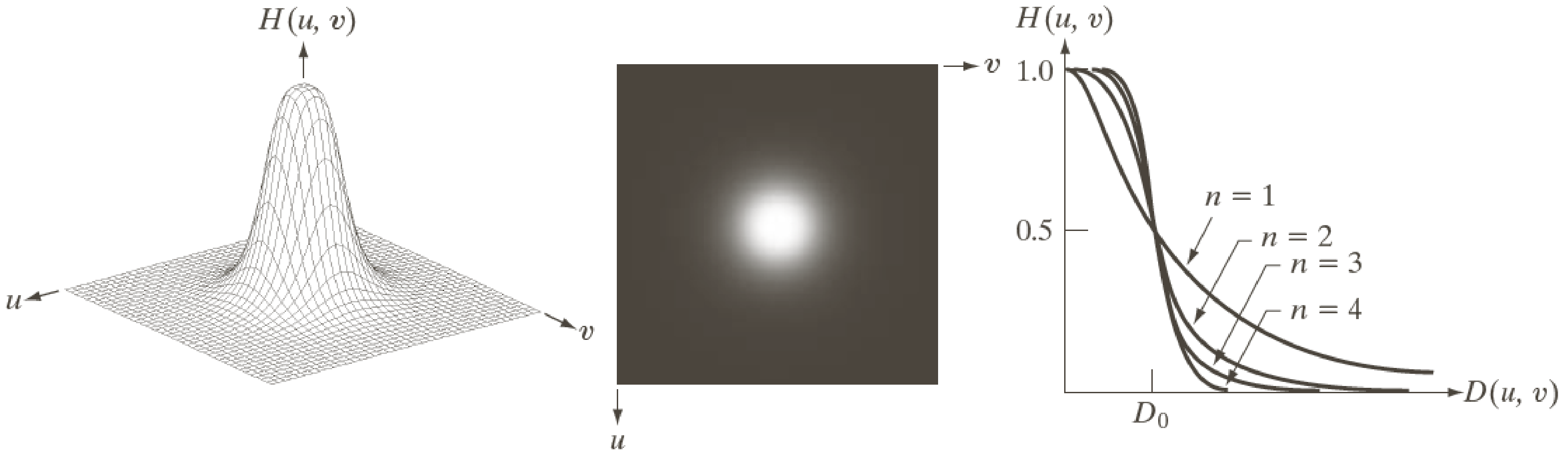

a b c

FIGURE 4.44 (a) Perspective plot of a Butterworth lowpass-filter transfer function. (b) Filter displayed as an image. (c) Filter radial cross sections of orders 1 through 4.

$$H(u,v) = \frac{1}{1+[D(u,v)/D_0]^{2n}}$$

→ order

D_0 is the cutoff frequency

Applying the BLPF

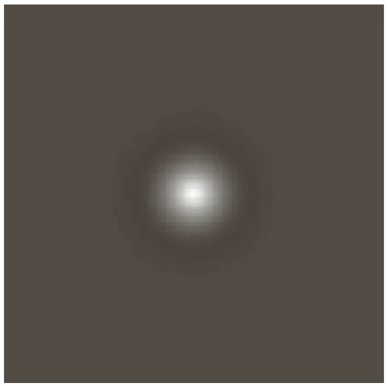

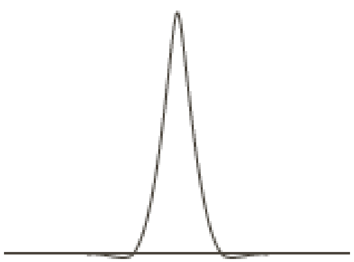

Order 2

Original

ILPF, cutoff 10
Energy 87%

ILPF, cutoff 30
Energy 93.1%

ILPF, cutoff 60
Energy 95.7%

ILPF, cutoff 160
Energy 97.8%

ILPF, cutoff 460
Energy 99.2%

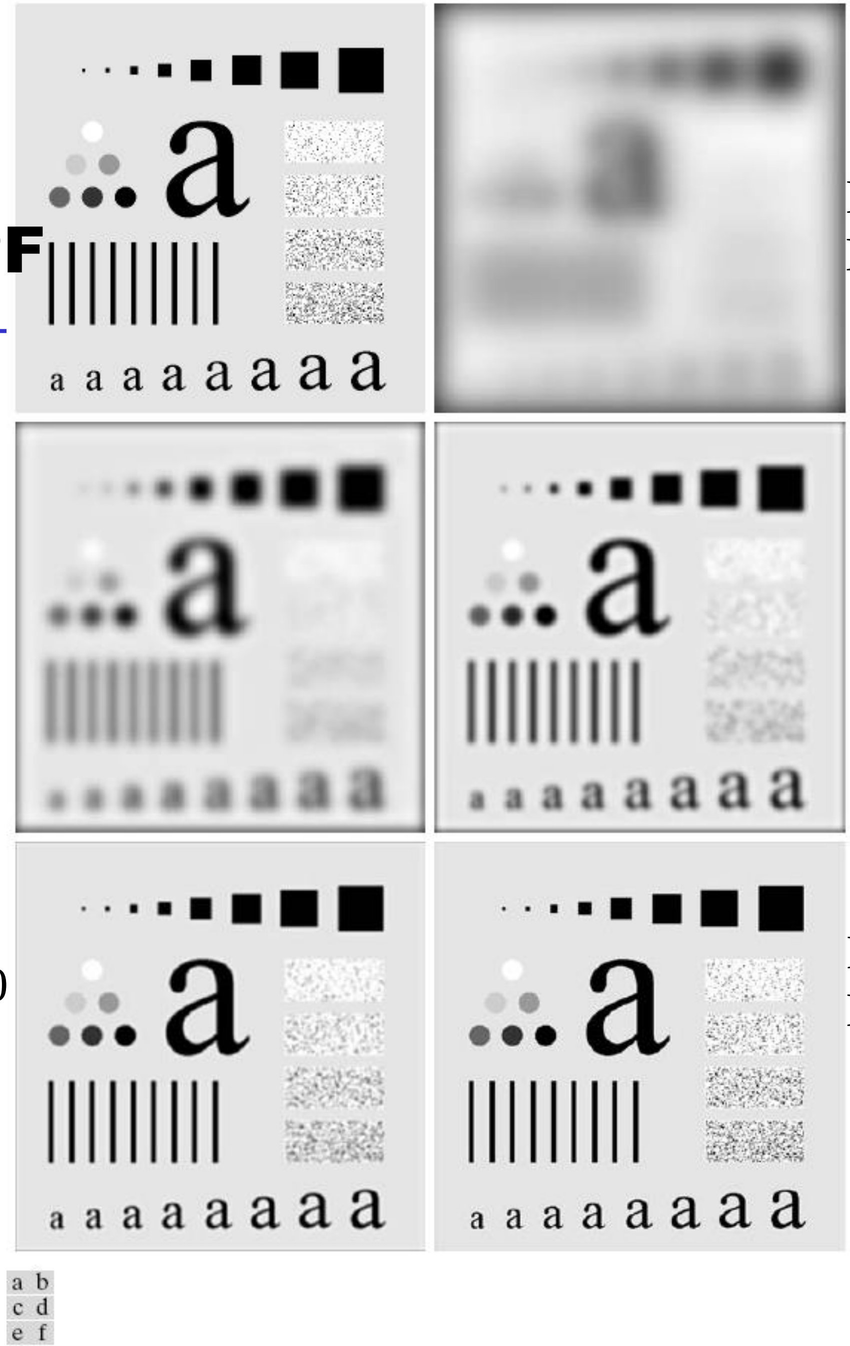

FIGURE 4.45 (a) Original image. (b)–(f) Results of filtering using BLPFs of order 2, with cutoff frequencies at the radii shown in Fig. 4.41. Compare with Fig. 4.42.

Different-Order BLPF

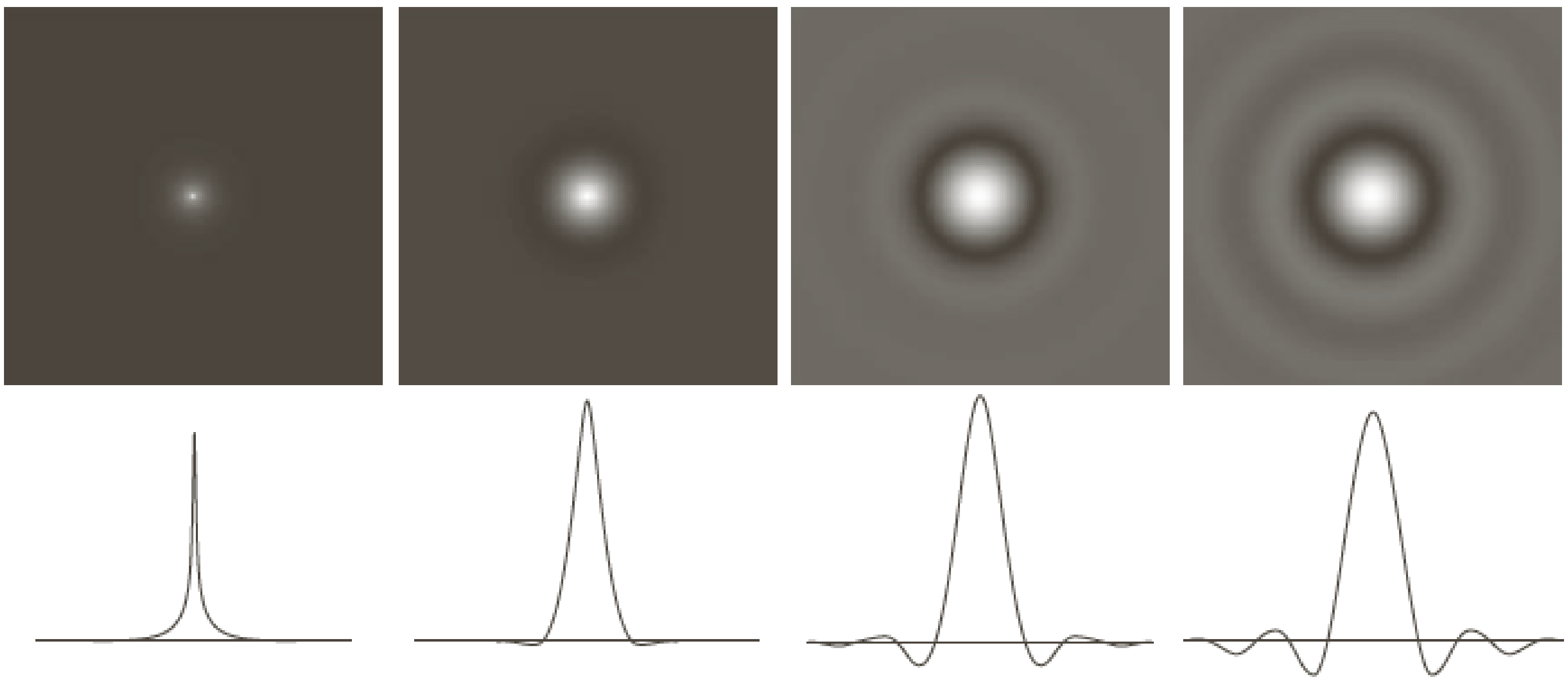

a b c d

FIGURE 4.46 (a)–(d) Spatial representation of BLPFs of order 1, 2, 5, and 20, and corresponding intensity profiles through the center of the filters (the size in all cases is 1000×1000 and the cutoff frequency is 5). Observe how ringing increases as a function of filter order.

Gaussian Lowpass Filters

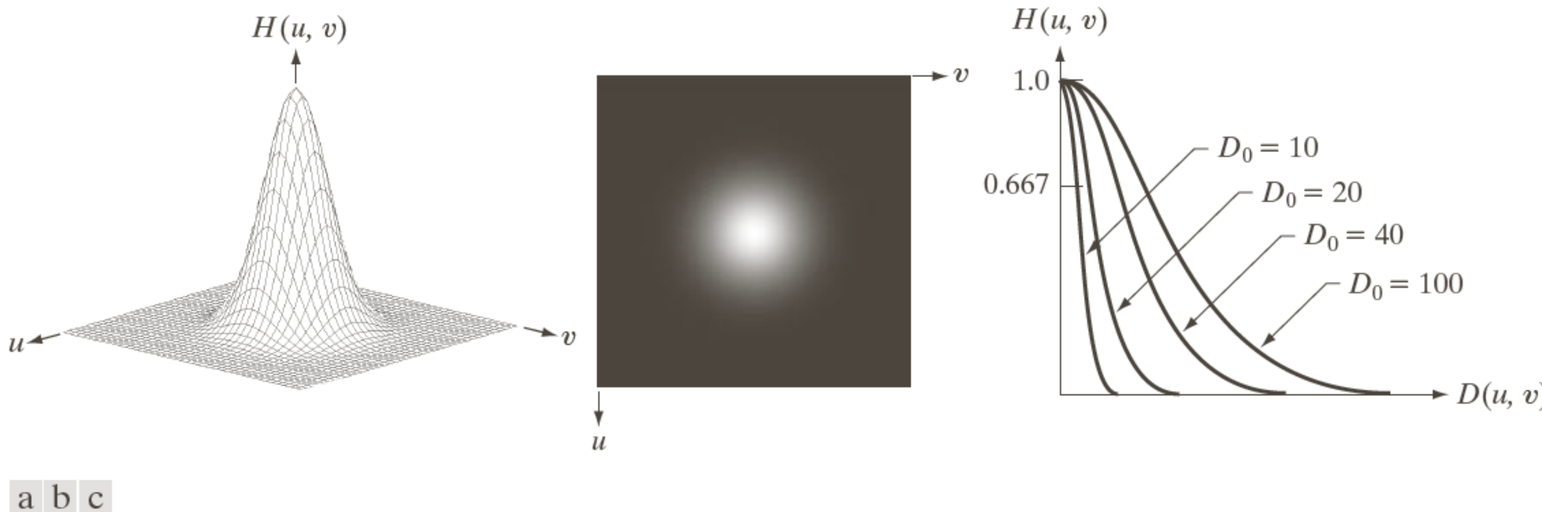

FIGURE 4.47 (a) Perspective plot of a GLPF transfer function. (b) Filter displayed as an image. (c) Filter radial cross sections for various values of D_0.

$$H(u,v) = e^{-D^2(u,v)/2D_0^2}$$

Applying the GLPF

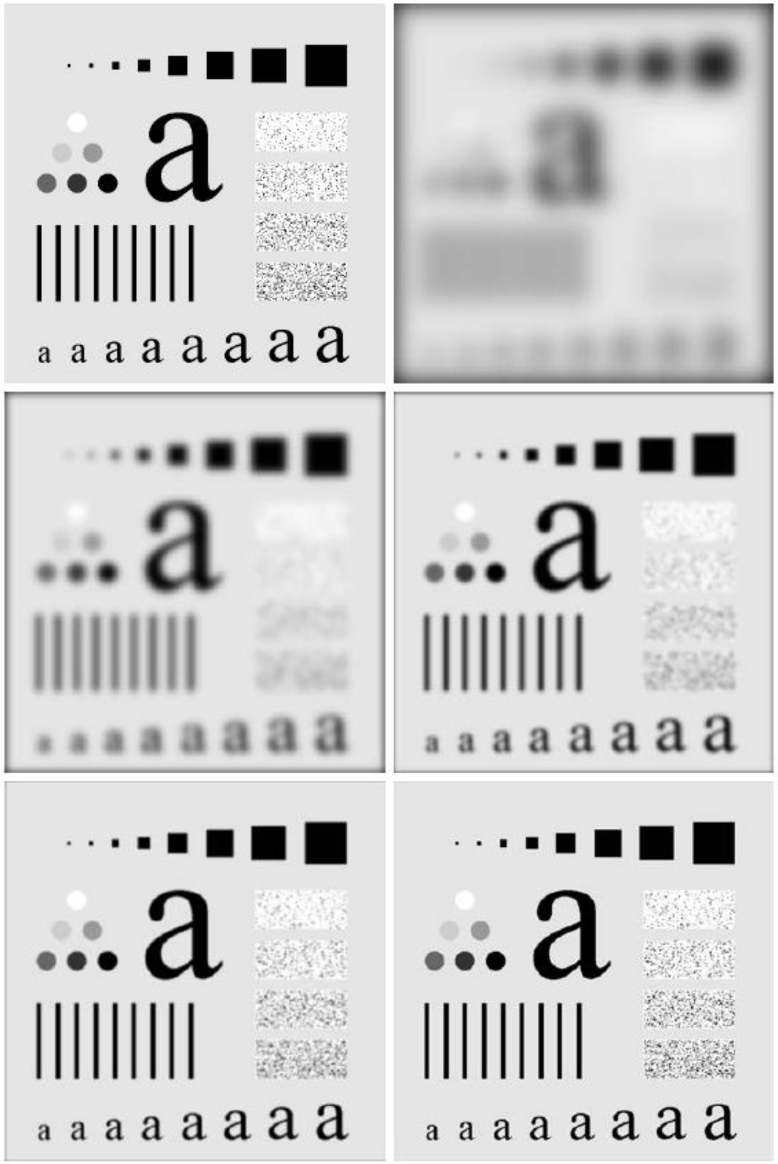

a b
c d
e f

FIGURE 4.48 (a) Original image. (b)–(f) Results of filtering using GLPFs with cutoff frequencies at the radii shown in Fig. 4.41. Compare with Figs. 4.42 and 4.45.